STUDY OF SEMICONDUCTING PROPERTIES OF SELECTED RARE-EARTH METALS AND COMPOUNDS

TECHNICAL DOCUMENTARY REPORT NO. AL TDR 64-239
October 12, 1964

Air Force Avionics Laboratory
Research and Technology Division
Air Force Systems Command
Wright-Patterson Air Force Base, Ohio

Project No. 4150, Task No. 415002

(Prepared under Contract No. AF 33(657)-10687,
BPSN: 36805-803A-415002, by
Battelle Memorial Institute, Columbus, Ohio;
J. F. Miller, F. J. Reid, L. K. Matson, J. W. Moody,
R. D. Baxter, and R. C. Himes, Authors)

DISTRIBUTION LIST

Cys	Activities at WPAFB
1	ASNXR
1	TDBTI
1	AVTM
5	AVTE
2	SEPI

Other DOD Activities

Cys	
1	AFSC (SCTA-4) Andrews AFB Wash DC 20331
1	OAR (RROSE) Bldg T-D Wash DC 20333
1	OAR (RROSL/LtCol Davies) Bldg T-D Wash DC 20333
1	OAR (RROSP Maj Bennett) Bldg T-D Wash DC 20333
1	ESD (ESRDL Maj VanHorne) L. G. Hanscom Field Bedford, Massachusetts
1	AFCRL (CRRES) L. G. Hanscom Field Bedford, Massachusetts
1	RADC (Documents Library) Griffiss Air Force Base, N. Y.
1	AMMTC (Tech Library) Patrick AFB, Fla.
1	AFSWC (SWOI) Kirtland AFB, N. Mex.
1	AU Library (7575) Maxwell AFB, Ala.

Other U. S. Govt. Agencies

Cys	
20	Defense Documentation Center Cameron Station Alexandria, Virginia 22314

Contractors

Cys	
1	Scientific & Tech Info Facility, NASA Representative (SAK DL) P. O. Box 5700 Bethesda, Maryland
1	Dr. F. V. Schossberger Armour Research Foundation 10 West 35th Street Chicago, Illinois
1	Dr. R. B. Biser Georgia Institute of Technology Atlanta, Georgia
1	Dr. E. V. Kleber Kleber Laboratories, Inc. P. O. Box 69 Burbank, California
1	American Potash & Chemical Corp. Lindsay Chemical Division Market Development Dept, Eastern Section 99 Park Avenue West Chicago, Illinois
1	Dr. G. L. Innes Michigan Chemical Corp. Rare Earths & Thorium Division St. Louis, Michigan
1	Dr. M. E. Caspari University of Pennsylvania Dept of Physics Philadelphia, Pennsylvania
1	Mr. Nathan Sclar Nuclear Corporation of America Central Electronic Mfg Division 2 Richmond Place Denville, New Jersey
1	Mr. Thomas Ramsey University of Texas Dept of Chemical Engineering Austin, Texas
1	Mr. M. Deckman, Allison Division General Motors Corporation Indianapolis, Indiana

FOREWORD

This final technical report was prepared by J. F. Miller, F. J. Reid, L. K. Matson, J. W. Moody, R. D. Baxter, and R. C. Himes of Battelle Memorial Institute, Columbus, Ohio, on Contracts AF 33(616)-7321 and AF 33(657)-10687, Project No. 4150, Tasks Nos. 41709 and 415002, respectively. The work was under the technical cognizance of Dr. C. R. Barnes of the Electronics Research Branch, Electronics Technology Division, Air Force Avionics Laboratory, Research and Technology Division, Air Force Systems Command, Wright Air Development Center.

ABSTRACT

This investigation was concerned with the compounding, crystal growth, characterization, and evaluation of compounds formed between the rare-earth elements and elements of chemical Groups V and VI. Special emphasis is placed on providing basic information to make possible the ultimate development of useful solid-state electronic devices based on these materials. In sampling the members of the rare-earth family, the elements cerium, neodymium, samarium, gadolinium, erbium, and ytterbium have been used in the preparation of representative compounds and alloys with anions, such as, selenium, tellurium, oxygen, arsenic, antimony, phosphorus, and nitrogen. Single crystal, bulk, and thin-film specimens have been prepared, and details regarding methods of compounding and crystal growth are given. Crystal structure and phase relationships indicate that, in some cases, as many as four distinct crystalline phases may exist within a single binary system. While electrical conductivities in the materials treated fall generally in the semiconductor range, transport mechanisms are not entirely consistent with classical semiconductor theory. The electrical properties of specimens of the various compounds and compositions are consistent, in general, with the present understanding of the chemistry and crystal structure of the rare-earth elements and compounds. In many cases it is evident that the presence of unfilled 4f shells, associated with the rare-earth elements, strongly influences electron transport in these materials, which fact is of both practical and theoretical interest. Several applications of rare-earth compounds and alloys studied are suggested. These include application in thermistors and related devices, adjustable-temperature-coefficient resistors, high-temperature thermoelectric generators, and active devices consisting of metal-insulator structures.

PUBLICATION REVIEW

Publication of this technical documentary report does not constitute Air Force approval of the reports findings or conclusions. It is published only for the exchange and stimulation of ideas.

FOR THE COMMANDER:

Robert D. Larson

ROBERT D. LARSON
Chief, Electronics Research Branch
Electronic Technology Division

TABLE OF CONTENTS

LIST OF FIGURES

LIST OF FIGURES
(Continued)

LIST OF TABLES

STUDY OF SEMICONDUCTING PROPERTIES OF SELECTED RARE-EARTH METALS AND COMPOUNDS

INTRODUCTION

This is the final Technical Documentary Report on the subject program and covers the research accomplishments from June 1, 1960, to December 31, 1963. The primary objective of this investigation is to develop new knowledge and control of the preparation and properties of selected rare-earth compounds through studies of the materials, ultimately as single crystals and films, and thus to assay the potential of these materials for electronic applications. To this end, a number of representative compounds and alloys of the rare-earth elements in combination with elements of chemical Groups V and VI have been investigated. Research has been conducted in the areas of compound preparation, purification, crystal growth and structure studies, film deposition, and electrical analysis.

Considering that there are 14 rare-earth elements, that information obtained in the early work pointed to the existence of several compounds in each of the systems, and that a number of Groups V and VI metalloid species are involved, the number of possible compounds in the systems under consideration is seen to be extremely large. To undertake investigation of all of the compounds would constitute a prohibitively large task. Therefore, available information on the chemistry of the rare-earth elements was utilized in the selection of representative compounds for study. In addition, since, in an initial exploratory study (Ref. 1)*, the more interesting electrical properties were observed for the selenides and tellurides, initial and major portions of this investigation were devoted to study of these compounds and their alloys.

In discussions of the chemistry of the rare-earth elements, the similarity of their behavior and the predominance of the tripositive oxidation state are often stressed – thus creating popular misconceptions. As shown in Table 1, other important oxidation states also are observed for a number of the elements. Conversion to the dipositive or tetrapositive state is, in fact, utilized in effecting the chemical separation of some elements from (naturally occurring) mixtures. Hence it is apparent that several types of chemical behavior of the rare-earth elements must be considered if one is to study representative rare-earth materials.

Among the tripositive ions, high stability is associated with the electronic configurations of the La^{3+}, Gd^{3+}, and Lu^{3+} ions in which the 4f levels are empty, half filled, and filled, respectively. The dipositive and tetrapositive oxidation states of the neighboring rare-earth elements (Table 1) appear to arise as a result of approach to, or achievement of, the stable $4f^0$, $4f^7$, $4f^{14}$ configurations. Among these, the dipositive states of samarium, europium, and ytterbium and the tetrapositive state of cerium are the more important; the corresponding states of thulium, praseodymium, and terbium appear to be less stable and are observed only under special conditions.

*References are given on page [illegible].

Manuscript released by the authors February 1, 1964, for publication as an AL FTDR Technical Documentary Report

TABLE I. OXIDATION STATES AND ELECTRONIC CONFIGURATIONS OF RARE-EARTH ELEMENTS

Element	Known Oxidation States	Corresponding 4f Electronic Configurations
La	3	$4f^0$
Ce	3 - 4	$4f^1$ - $4f^0$
Pr	3 - 4	$4f^2$ - $4f^1$
Nd	3	$4f^3$
(Pm)	3	$4f^4$
Sm	2 - 3	$4f^6$ - $4f^5$
Eu	2 - 3	$4f^7$ - $4f^6$
Gd	3	$4f^7$
Tb	3 - 4	$4f^8$ - $4f^7$
Dy	3	$4f^9$
Ho	3	$4f^{10}$
Er	3	$4f^{11}$
Tm	2 - 3	$4f^{13}$ - $4f^{12}$
Yb	2 - 3	$4f^{14}$ - $4f^{13}$
Lu	3	$4f^{14}$

Within a given class of compounds, it is reasonable to expect that different characteristics will be obtained as the chemical nature of the rare-earth element changes. Accordingly, rare-earth elements were selected from the three types noted. Neodymium, gadolinium, and erbium were chosen as representatives of the "regular", rare-earth elements which exhibit only the tripositive oxidation state. Samarium and ytterbium were selected for study as representatives of the elements which exhibit both dipositive and tripositive states. Compounds of cerium were also prepared and studied, since this element exhibits both the tripositive and tetrapositive states.

Another factor which one might expect to warrant consideration is the possible effect of the lanthanide contraction. The decrease in atomic and ionic radii with progression through the rare-earth series certainly produces an effect on properties of the elements and compounds. However, results indicate this to be of secondary importance among the effects and phenomena noted and discussed.

COMPOUND PREPARATION AND CRYSTAL GROWTH

The principal technique employed for compound synthesis has been a solid-vapor reaction between rare-earth-metal filings and vapors of the Group V or Group VI element at relatively low temperatures (450 to 1050 C). This reaction yields the materials in granular form from which bulk crystalline specimens are prepared by melting techniques or by powder-metallurgical techniques. Although the majority of the materials studied were prepared by this solid-vapor reaction, employed in special cases were other synthetic techniques such as liquid-vapor reactions and solid-vapor

reactions in which the solid was the bulk or thin-film rare-earth metal. A discussion involving thin films of rare-earth metals and compounds is found in a later section on "Thin Films".

Three general methods of crystal growth have been investigated: (1) growth from stoichiometric or nearly stoichiometric melts, (2) growth by vapor deposition, and (3) growth from solution. Study of the low-temperature crystal-growth methods, items (2) and (3), was attractive, since the preparation of purer, more nearly perfect crystals through reduction of contamination and attainment of better control over the crystallization process should be possible at the low temperatures.

Vapor-Solid Reaction

In the most successful method developed to date for the preparation of bulk specimens, the compound is first prepared in powder or granular form. The granular material is then melted down and cast into an ingot from which bulk specimens suitable for evaluation can be obtained.

The compounds were prepared in granular form by reacting vapor of the Group V or Group VI element with filings of the rare-earth metal at moderate temperatures. Some contaminants were probably introduced in producing the filings. However, the increased reaction rate obtained thereby is believed to outweigh the contamination effects, at least in an exploratory program.

The vapor-solid reactions were carried out in sealed, evacuated Vycor tubes, which were designed so as to maintain physical separation of the rare-earth metal and the Group V or Group VI element in the condensed state. Maintaining this physical separation precludes the possibility of the rapid, violent reaction which tends to take place on direct contact of the condensed phases. For example, the reaction between dysprosium and selenium has been observed to reach explosive proportions at about 400 C.

To carry out the desired reaction, vapor of the Group V or Group VI metal was distilled over rare-earth-metal filings at temperatures in the range 450 to 1050 C. The reaction conditions were varied somewhat, depending on the specific reaction being carried out. In general, temperature was increased slowly in a period of 4 to 50 hours, and was held at the selected level for an additional 14 to 150 hours. Periodic checks were made to determine when the reaction was complete. The reaction was considered to be complete when (1) a condensate of the volatile constituent failed to form on the reaction-tube wall as it cooled after being removed from the furnace, and (2) the product had a homogeneous appearance (i.e., contained no visible particles of partially reacted or unreacted metal). In the first experiments on the preparation of a given compound, the approximate minimum thermal treatment required for synthesis was thus determined empirically; these conditions then were duplicated or exceeded in subsequent preparations.

The reaction conditions varied widely as the identity of the compound being prepared changed. For example, the temperature was increased more slowly when a high-vapor-pressure element such as selenium was involved than for initiation of a reaction

involving a low-vapor-pressure element such as bismuth. Likewise, the longer reaction times and higher temperatures generally were required for reactions of the latter group involving the less volatile metalloids. This is amply illustrated by comparison of the reaction between yttrium and bismuth, which required 140 hours at 800 to 900 C, with that between dysprosium and selenium to form the sesquiselenide, which appeared to be complete in approximately 6 hours at 400 C. Other examples of reaction conditions employed are given in Table 2.

As is indicated in the preceding discussion, the vapor-solid reaction has been investigated for the preparation of a number of classes of rare-earth intermetallic compounds. Several general observations can be made regarding application of the procedure to the synthesis of compounds of the various classes. Although the observations are based on work with just a few representative systems, it is reasonable to expect that similar behavior will be exhibited in nearly all the subject binary systems. In the majority of the cases, the reactions to form the compounds in a powdered or granular state were carried out in evacuated, sealed, fused silica or Vycor ampoules. In such containers, it was necessary that the maximum reaction temperature be held at 900 C or lower, since it was noted that the rare-earth metal and/or compounds react with the fused silica at higher temperatures. X-ray diffraction studies on the Gd-Te system showed that single-phase specimens of compositions in the M_3X_4 to M_2X_3 range can be prepared directly in the granular form by the vapor-solid reaction at temperatures $\leq$ 900 C. The compositions corresponding to the monotelluride, however, are not converted to the compounds by similar treatment; in these cases, the particles are observed to consist of unreacted centers of gadolinium metal covered with surface layers of a phase having the (M_3X_4-M_2X_3) structure. Conversion to the monotelluride was observed to have occurred only after the material had been subjected to higher temperatures ($\geq$ 1300 C). This usually was accomplished in the course of the subsequent melting of the granular materials. Hence, no attempt was made to determine the low-temperature limit for the transition.

The solid-vapor reaction also has been used for the preparation of rare-earth bismuthides, antimonides, arsenides, phosphides, and nitrides, in granular form, as indicated in Table 2. The reactions between the rare-earth metals in finely divided form and the elemental vapors of the metalloids, bismuth, antimony, arsenic, and phosphorus, seemed to proceed at reasonable rates to form the 1:1 compounds having the fcc, NaCl-type structure. To prepare the nitride, however, it was necessary that a nitrogen compound (ammonia) be used as a source of reactive nitrogen.

The various reactions also were attempted using bulk specimens of the rare-earth metals rather than the small particles (filings). Since only thin surface layers of the majority of the compounds (specifically, the selenides, tellurides, antimonides, and phosphides) were formed, the results suggested that, in most cases, the reaction rates may be limited by the rates of diffusion of the metalloid species through the initially formed layers of the product compounds. An exception to this was encountered in the arsenides. It was possible to prepare bulk specimens of the arsenides (e.g., YAs, GdAs, NdAs) by diffusing arsenic into sizable solid specimens of the rare-earth metals at moderate temperatures. To illustrate, arsenic (vapor at 1 atmosphere of pressure) diffused into and reacted with solid neodymium metal at 1100 C so rapidly that the compound which formed spalled off and the solid disintegrated. At 750 C and with arsenic vapor pressure at 0.02 atmosphere, however, the reaction rate was lower and solid specimens of NdAs were obtained.

TABLE 2. TYPICAL CONDITIONS FOR PREPARATION OF COMPOUNDS BY THE SOLID-VAPOR REACTION

Synthetic Composition	Reaction Temperature, C	Time, hours
Nd_2Te_3	25-800	4
	800	156
Nd_3Te_4,	25-700	4
Gd_2Te_3	700	12
	800	144
Nd_3Se_4	25-350	2
	350	10
	400	17
	450	74
Nd_2Se_3	25-300	6
	300	12
	350	4
	400	5
	450	14
NdSb	25-600	14
	600	123
NdAs,	25-500	8
SmAs	500	15
	600	20
	680	20
NdP	25-900[a]	24
	900	32
	1050	72
NdN	1000[b]	125

(a) Pressure of phosphorus vapor held at ~1 atm by use of two-furnace technique.
(b) Vapor phase = anhydrous NH_3.

Vapor-Liquid Reactions

A number of compounds have been prepared by reacting vapor of the Group V or Group VI species with the molten rare-earth metal. These reactions are carried out in evacuated, sealed quartz or Vycor tubes. Induction heating is used to melt the rare-earth metal, which is placed in a boat (container materials are discussed later in this section) within the sealed quartz envelope. The remainder of the quartz envelope is heated, usually with electric furnaces, so as to create and maintain a suitable concentration of vapor of the Group V or Group VI species.

The vapor-liquid reaction has been carried out in two different ways, both of which yield bulk specimens of the compounds. In both of the methods, an excess of the Group V or Group VI species is used, and vapor pressure of this component is controlled by controlling minimum temperature of the condensed excess. In the first, the ingot of rare-earth metal is melted and maintained at a temperature just above its melting point. Minimum temperature of the quartz envelope is then gradually increased so as to slowly increase concentration of the vapor of the Group V or Group VI species. As concentration of the vapor is increased, the compound crystallizes first in the cooler regions of the inductively heated melt and, under proper conditions, the solid-liquid interface progresses gradually toward the high-temperature regions (Ref. 2). In the second method, the ingot of rare-earth metal is melted and maintained at a temperature just above the melting point of the compound being synthesized. Pressure of the vapor of the Group V or Group VI species is then made equal to decomposition pressure of the compound (at its melting point) by raising the minimum temperature of the quartz envelope to a suitable value. Progressive crystallization of the compound is accomplished by withdrawing the (molten) ingot laterally from the induction coil.

In carrying out the vapor-liquid reactions, a container problem has been encountered. Whereas tantalum apparently is a satisfactory container for simple melting of the compounds, the tantalum boats are severely attacked during prolonged periods of exposure to selenium, tellurium, or antimony vapor. Graphite containers, which are not noticeably attacked by Group V or Group VI vapors or by the molten compounds, are attacked by the molten rare-earth metals. In the course of the work, a number of container materials have been investigated. A listing of these materials and observations as to their shortcomings are given in Table 3. There has been no visual evidence of reaction between magnesia containers and the melts of the rare-earth metals or compounds. However, some difficulty has been experienced with regard to fracturing of the containers. It appears that this can be eliminated by avoiding thermal-shock stresses.

Growth From a Melt

In efforts to develop methods for crystallizing sound bulk specimens and, ultimately, for growth of single crystals of these high-melting materials, a number of methods have been investigated. The basic methods, involving growth from a melt, include the vertical Bridgman method, button casting, zone melting, and czochralski or "crystal-pulling" methods.

Ingots cast by the Bridgman method almost invariably contained voids, presumably resulting from the entrapment of pockets of foreign gases or metalloid vapor in the

TABLE 3. EVALUATION OF CONTAINER MATERIALS FOR COMPOUND SYNTHESIS

Container Material	Observation
Graphite	Attacked by molten rare-earth metal; appears to be satisfactory for short-term use with molten compounds
Tantalum	Attacked by vapor of Group V or Group VI elements; appears to be satisfactory for short-term use with compounds
Alumina	Attacked by molten rare-earth metals; subject to fracture by thermal-shock stresses
Boron nitride	Attacked by molten rare-earth metals; hydrolyzes slightly in normal atmosphere
Titanium diboride	Attacked by molten rare-earth metals
Magnesia	No evidence of attack by molten rare-earth metals, vapor of Group V or Group VI elements, or molten compounds; molten compounds diffuse through ceramic sections; subject to fracture by thermal-shock stresses

crystallizing material. Some fracturing of the ingots also occurred, which apparently resulted from compressive stresses imposed by the container wall.

Improvement in both respects was expected for button-cast specimens because of the large exposed surface area, which should favor expulsion of gases, and lack of a constraining container wall, which should minimize compressive stresses. However, specimens which were cast in this way contained numerous voids and were fractured throughout. The poor results are believed to be due to extremely steep thermal gradients which were present under the experimental conditions prevailing.

Zone melting in an open boat did not yield good specimens. Again, the extremely steep thermal gradients developed appeared to have a detrimental effect. Although graphite has appeared to be satisfactory as a container material in short-term use, appreciable reaction is observed between the graphite and the melt in the long-term zone-melting runs. Ingots which were zone melted in graphite were bonded to the container and were fractured throughout, presumably because of the difference in thermal expansion of the two materials.

In initial attempts to zone melt in tantalum boats, one difficulty was encountered. In the molten state, the materials "wet" the tantalum and "creep" up over the side of the boat, leaving only a thin layer of sample in the boat. One solution to this problem lies in the use of a tubular container.

A tubular container has been used for the zone melting and zone crystallization as shown in Figure 1. The melting and crystallization are done in a tantalum "test tube" which is placed within a long tubular susceptor. The apparatus is set up so that the longitudinal axis of the test tube is tilted from the horizontal. Directional crystallization is caused to occur by moving the container slowly through the rf coil. Direct induction heating of the tantalum test tube is possible, but better results have been obtained when a tubular susceptor was used as shown.

This relatively simple setup is seen to have several advantages. The crystallization process can be observed directly through the viewport in the end of the tube. Crystallization can be initiated in the small "tip" which is formed at the shallow end of the melt. Such a procedure promotes growth of single, or large, crystals. No significant compressive stresses, which cause fracturing, are imposed on the ingot by the container if melt level is kept below the midplane of the tube. Usually no difficulty is experienced in removing the ingot from the container following the run.

Crystallization by the simple technique described has consistently yielded sound ingots of a number of rare-earth materials, some of which were single crystals and most of which contained relatively large crystals. Voids and fractures have been virtually eliminated. The combination of the large exposed surface area and a favorable thermal pattern is apparently conducive to evolution of the gases (or vapors) which caused voids to form when other techniques were employed.

The melting points of the samarium and ytterbium monoselenides and monotellurides are high, ca. 2000 C. At these temperatures the materials "wet" the tantalum containers, and thin sections, such as are obtained from the tilted-tube zone melting procedure fracture on cooling. However, the slow cooling of melts contained in upright 3-inch-high tantalum crucibles has yielded a number of ingots which contain large single-cyrstal sections. The melting is done in argon using a 4-inch-long, 10-turn

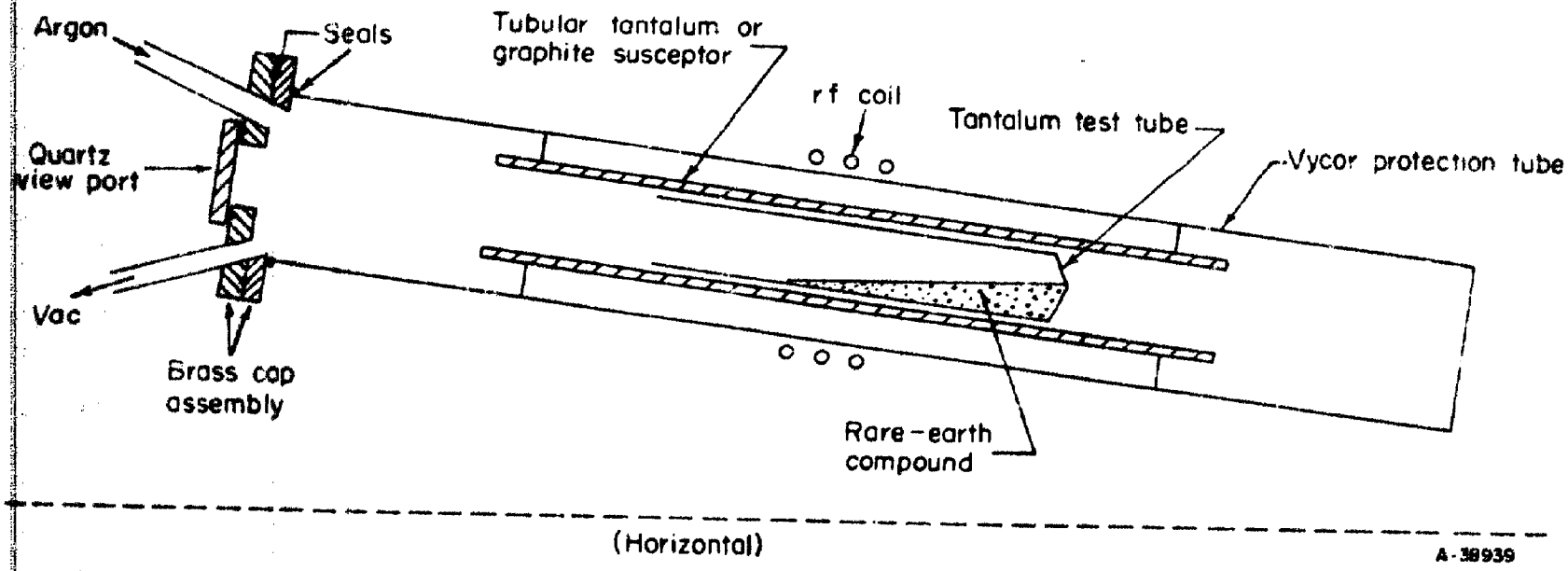

FIGURE 1. SCHEMATIC OF APPARATUS FOR ZONE MELTING

induction coil. Temperature of the melt is decreased gradually through the freezing point by gradual reduction of output of the rf generator. Typical rates of decrease were 20 C per minute in the range >2000 to ~1000 C. Single-crystal specimens, such as those shown in Figure 2 which are large enough for use in electrical-property studies, can be cleaved from the ingots. Table 4 shows the melting-temperature ranges applicable to the growth of sound specimens of various rare-earth compounds and alloys from the melt.

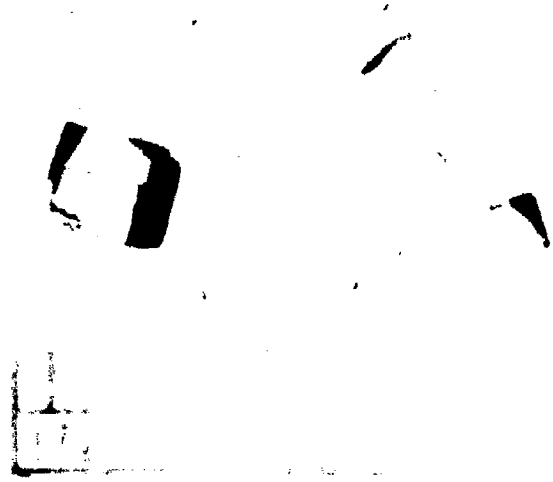

FIGURE 2. SINGLE-CRYSTAL SPECIMENS CLEAVED FROM INGOT OF MELT-GROWN SmSe

Crystal-pulling experiments were carried out on gadolinium and neodymium tellurides in both a "standard" Czochralski and a sealed Gremmelmaier-type magnetic crystal puller. Runs were made in argon, helium, and tellurium vapor atmospheres. The melts, which were contained in tantalum crucibles, were heated inductively. Seed rods were of tantalum or graphite.

The experiments failed to yield sound, coherent ingots. In all experiments, heavy deposits which formed on the crystal puller wall seriously hampered the work; this was most severe in the attempted pull of Gd_2Te_3 in tellurium vapor. In the case of the Gd-Te compounds, a crust which interfered with the crystal-growth process formed on the surface of the melt. This crust appeared to be formed of loosely bonded particles of materials or phases which were higher melting than the main portion of the charge. Loss of tellurium from the surface layers or the presence of high concentrations of impurities could account for the crust formation. In view of the generally discouraging results of the experiments, no analyses were made to check this.

In experiments with the Nd-Te compounds, "clean" melt surfaces were obtained, and it was possible to crystallize short, irregularly shaped ingots. However, in both systems (Gd-Te and Nd-Te), the material seemed to melt and freeze over a range of

TABLE 4. MELTING-TEMPERATURE RANGES FOR RARE-EARTH COMPOUNDS AND ALLOYS

Composition	MTR[a], C	Composition	MTR[a], C	Composition	MTR[a], C
GdTe	1840-1900	CeTe	<1890	$Nd_{0.02}Sm_{0.98}Se$	1830-1900
Gd_3Te_4	~1410	$CeTe_{1.4}$	1450-1550	$Nd_{0.08}Sm_{0.92}Se$	1800-1900
$GdTe_{1.4}$	1400-1460	$CeTe_{1.46}$	1480-1640	$Nd_{0.11}Sm_{0.89}Se$	1850-1880
$GdTe_{1.46}$	1400-1480	Ce_2Te_3	1660-1800	$Nd_{0.13}Sm_{0.87}Se$	1850-1860
Gd_2Te_3	1500-1510	YbTe	1720-1760	$Nd_{0.16}Sm_{0.84}Se$	1800-1850
				$Nd_{0.24}Sm_{0.76}Se$	1800-1840
GdSe	1860-1865	$CeSe_{1.40}$	1850-1900	$Nd_{0.33}Sm_{0.67}Se$	1870-1940
Gd_3Se_4	1500-1620	$CeSe_{1.44}$	1970-2040		
$GdSe_{1.4}$	1510-1680	$CeSe_{1.47}$	1980-2040	$Ce_{2.5}Ba_{0.5}Te_4$	1420-1530
$GdSe_{1.46}$	1540-1680	Ce_2Se_3	1600-2050	$Ce_{2.5}Ba_{0.5}Se_4$	1690-1800
YbSe	1940-1950	$CeSe_2$	1200-1500	$Ce_{2.3}Ba_{0.7}Se_4$	1650-1730
GdAs	>2200	ErAs	>2500	$Gd_{2.5}Sr_{0.5}Se_4$	1640-1680
NdTe	2020-2070	$Ce_{2.5}Sr_{0.5}Te_4$	1400-1500	$Nd_{0.55}Sm_{0.45}Se$	~1860
Nd_3Te_4	1630-1690	$Ce_{2.5}Sr_{0.5}Se_4$	1600-1700	$Nd_{0.67}Sm_{0.33}Se$	~1860
Nd_2Te_3	~1650	$Ce_{2.38}Sr_{0.62}Se_4$	1810-1840	$Nd_{0.84}Sm_{0.16}Se$	1840-1880
SmTe	1910-1930	$Ce_{2.25}Sr_{0.75}Se_4$	1600-1830		
Sm_2Te_3	1410-1530	Ce_2SrSe_4	1600-1910	$Nd_{0.02}Yb_{0.98}Se$	2020-2070
				$Nd_{0.08}Yb_{0.92}Se$	<2100
Sm_4Se_3	1900-2000			$Nd_{0.33}Yb_{0.67}Se$	<1980
SmSe	~2100				
Sm_2Se_3	1540				
CeSe	~1820				
Ce_3Se_4	1560-1800				
NdAs	>2100				

(a) MTR, i.e., temperature range within which melting was observed to occur.

temperatures* rather than at a discrete melting point. As a result, large portions of the pulled material frequently remelted and dropped away from the ingot back into the melt; because of this, no sizable ingots or crystals were obtained. Deviations from a given stoichiometry or relatively low purity could account for the observed behavior. This method of crystal growth finally was abandoned.

Growth By Vapor Deposition

Experiments on the low-temperature vapor-phase growth of crystals of Gd_2Te_3 and Nd_2Te_3 have been moderately successful. Sizable crystals of $GdTe_2$ and small needlelike crystals of Gd_2Te_3 of good physical quality have been prepared by the vapor method.

In the vapor-growth work, the sealed-system method has been utilized. Specimens of rare-earth telluride plus a small quantity of elemental halogen (I_2) or a source of halogen (e.g., NH_4I, NH_4Cl) were sealed in evacuated quartz tubes. Alternatively, elements in the proper proportions to yield rare-earth tellurides were used as starting materials. The majority of the experiments to be discussed were of this type. In these cases, the standard procedure for low-temperature vapor-solid reactions was used to form the compound prior to the vapor-growth run. Two bases were used for addition of the halogen: charges were made up to correspond to initial compositions of the types (1) x RE_2Te_3 + y REX_3, or (2) x RE_2Te_3 + y X_2. As is indicated in Table 5, various concentrations of halogen, corresponding to those required for reaction with 1 to 20 atomic per cent of the rare-earth metal present to form REX_3, were used in both types of additions. Vapor growth was carried out by placing the sample tube in a temperature gradient. Maximum temperature was varied between 820 and 1045 C. Minimum temperature was varied between ~200 and 910 C. Vapor-growth time ranged from 39 to 288 hours, and both horizontal and vertical systems were used. In the vertical furnace, a temperature inversion was used, i.e., the higher temperature was at the bottom and the lower temperature at the top of the tube.

Small acicular crystals of the Gd_2Te_3 phase, ~0.5 mm across and up to 5-mm long, were grown by use of charges containing low concentrations of halogen (i.e., on the basis of GdI_3 formation, equivalent to $\leq$ 5 atomic per cent of the gadolinium metal present), as is indicated in the data for Experiments 37, 56, 39 (Table 5). Although the crystals were small, results of X-ray diffraction analyses indicated that they were of good physical quality. Single-crystal X-ray diffraction patterns obtained with them were much sharper than those previously obtained with material crystallized from the melt. As a result, it was possible to index structure of the Gd_2Te_3 phase (orthorhombic with unit cell constants a = 11.83 A, b = 12.01 A, c = 4.28 A). The c-axis was found to be parallel to the needle axis in the vapor-grown crystals.

Fairly large platelets of $GdTe_2$, up to ~5 mm by 5 mm by 3 mm thick as shown in Figure 3, were grown by use of charges containing higher concentrations of halogen (i.e., on the basis of GdI_3 formation equivalent to $\geq$ 5 atomic per cent of the gadolinum metal present; see Experiments 56, 57, 41 in Table 5). Physical quality of these crystals also appeared to be good. Several of the crystals were large enough to yield single-crystal Hall specimens. Comparison of results of electrical measurements on

*, a behavior similar to that of impure metals which are said to have a "hot-short" range.

melt-grown and vapor-grown $GdTe_2$ (see Table 13 in section on "Electrical Properties") indicates that the latter material is of better quality also. Measurable Hall effect and carrier mobility were observed only for the vapor-grown material.

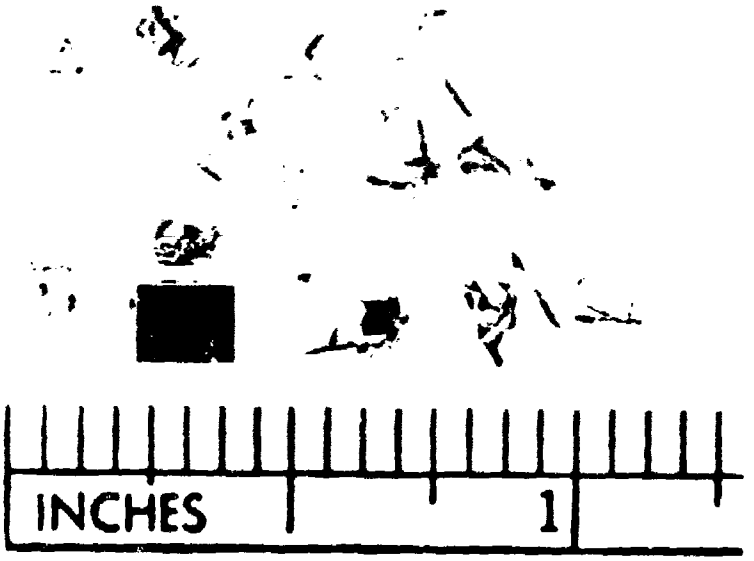

FIGURE 3. VAPOR-GROWN SINGLE CRYSTALS OF $GdTe_2$

Significant rates of crystal growth were obtained in vertical, but not in horizontal systems, presumably because conditions are more favorable for convection currents (and material transport therein) in the former case. Run times in excess of 200 hours were required to obtain significant amounts of crystal growth. When excess iodine was added, as in the first group of experiments in Table 5, appreciable concentrations of free tellurium were present (e.g., $3I_2 + Gd_2Te_3 \rightleftharpoons 2GdI_3 + 3/2\ Te$) and the higher tellurides, $GdTe_2$ and $GdTe_4$, tended to form readily. For example, high concentrations of $GdTe_4$, which is bronze colored and therefore readily identified, were present in the feed stocks of Experiments 46 and 54 following the runs. No appreciable vapor transport was obtained in cases in which ammonium halides were used.

Appearance and characteristics of the residual feed stocks, particularly for charges containing the higher concentrations of halide or halogen, suggested that halide-telluride solid solutions may have formed gradually, thus reducing activity of the halide and hence its effectiveness as a vapor-transport agent. Homogeneous-appearing, soft, brown crystalline masses (in contrast to the hard, metallic gray or black of the Gd_2Te_3 and $GdTe_2$ phases) formed, which, when heated strongly with a torch in vacuum, dissociated into (clear) GdI_3 and dark (Gd-Te) phases.

Although the data presented in Table 5 do not clearly so indicate, best results were obtained with charges of presynthesized compound and with the lower concentrations of halogen.

TABLE 5. SUMMARY ON VAPOR GROWTH

...riment	Composition of Main Charge	Halogen Added As	Upper Limit of Halide Concentration[a]	Temperature, C	Time, hr	Furnace Gradient	Vapor-Deposited Crystals
31	Gd_2Te_3	Excess I_2	Trace (<<1)	850-950	144	Vertical	Gd_2Te_3 needles
41	Gd_2Te_3	Excess I_2	1	850-950	45	Horizontal	None[b]
43	Gd_2Te_3	Excess I_2	5	850-950	92	Horizontal	None
36	Gd_2Te_3	Excess I_2	5	840-920	234	Vertical	Initially, Gd_2Te_3 needles; later, overgrowths of GdTe platelets
40	Gd_2Te_3	Excess I_2	20	850-950	92	Horizontal	None
34	Gd_2Te_3	Excess I_2	20	840-925	172	Vertical	None
40	Gd_2Te_3	GdI_3	1	800-900 850-950	23 16	Horizontal	None
39	Gd_2Te_3	GdI_3	5	850-950	76	Vertical	Some Gd_2Te_3 needles
57	Gd_2Te_3	GdI_3	10	910-1045 810-945	127 64	Vertical	Some $GdTe_2$ platelets
41	Gd_2Te_3	GdI_3	20	850-950	260	Vertical	Large platelets of $GdTe_2$ (see Figure 2)
46	Gd_2Te_3	NH_4I	Trace (<<1)	675-860 770-955 925-1030	178 144 15	Vertical	None
54	Gd_2Te_3	NH_4Cl	5	850-950 100-950	63 144	Vertical	None
62	GdTe	GdI_3	5	810-945	40	Vertical	Film formed on reaction tube wall; not one of known Gd-Te compound phases; not identified
58	Nd_2Te_3	NdI_3	10	810-945	246	Vertical	None
63	Nd_2Te_3	NH_4I	Trace (<<1)	850-950	288	Vertical	None

[a] Atomic per cent of rare earth metal present which would be present as REX_3 assuming complete reaction.
[b] No appreciable crystal growth.

The method appears to be particularly useful for the preparation of polyselenides and polytellurides. However, growth rates are very low. Control of stoichiometry for the preparation of other compounds may not be practical.

Growth From Solution

Exploratory experiments on the growth of crystals of the sesquitellurides from solution were carried out with Gd_2Te_3. The telluride was found to be soluble in the anhydrous halides, $GdCl_3$ and GdI_3, which were selected as solvents. However, crystals of the sesquitellurides were not obtained from such solutions.

In the initial exploratory experiment, a specimen of Gd_2Te_3 was placed in a quantity of anhydrous $GdCl_3$ (melting point, 609 C). The temperature was raised to effect solution, then was lowered until recrystallization occurred. As the temperature was increased (to 900 C), the Gd_2Te_3 dissolved and tellurium vapor appeared in the free space above the melt in the sealed quartz tube. As the solution was cooled, very small dark, needlelike crystals were precipitated. These were found by X-ray analysis to be crystals of the $GdTe_2$ phase. Since the temperature-composition studies had shown that formation of the desired Gd_2Te_3 phase would be favored by use of higher temperatures, GdI_3 (melting point, 926 C) was used as the solvent in subsequent experiments.

Experiments with GdI_3 as the solvent were run in both horizontal and vertical systems. A solution of 25 mole per cent Gd_2Te_3 in GdI_3 was directionally frozen at a linear rate of 1/4 inch per hour in a horizontal quartz tube. A solution of 30 mole per cent Gd_2Te_3 in GdI_3 was crystallized by a Bridgman drop (vertical) at a rate of 1/16 inch per hour. Both experiments yielded similar polycrystalline ingots which, by hardness checks, appeared to be uniform along their length, indicating that little or no precipitation or segregation of Gd_2Te_3 had occurred. The materials, similar in appearance to the residual feed stocks from vapor-growth experiments, again suggest that telluride-halide solid solutions probably were formed.

STRUCTURE AND PHASE RELATIONSHIPS

In the course of studies directed toward understanding and control of the electrical properties of rare-earth compounds, some study has been made of crystalline phases and phase-temperature-composition relationships in the systems involved. In order to discern more general relationships among the compositions, crystal-structure data, and electrical properties, literature data have been considered as well.

Data obtained in the course of the work (some of which are presented in Figures 4 and 5) indicate that there are typically at least four crystalline phases in the binary systems containing a Group VI element such as selenium or tellurium. These are: (1) a high-melting MX compound, (2) an M_3X_4-M_2X_3 phase which persists through the composition range indicated, and (3 and 4) several compounds containing higher concentrations of metalloid, such as $GdTe_2$ and $GdTe_4$.

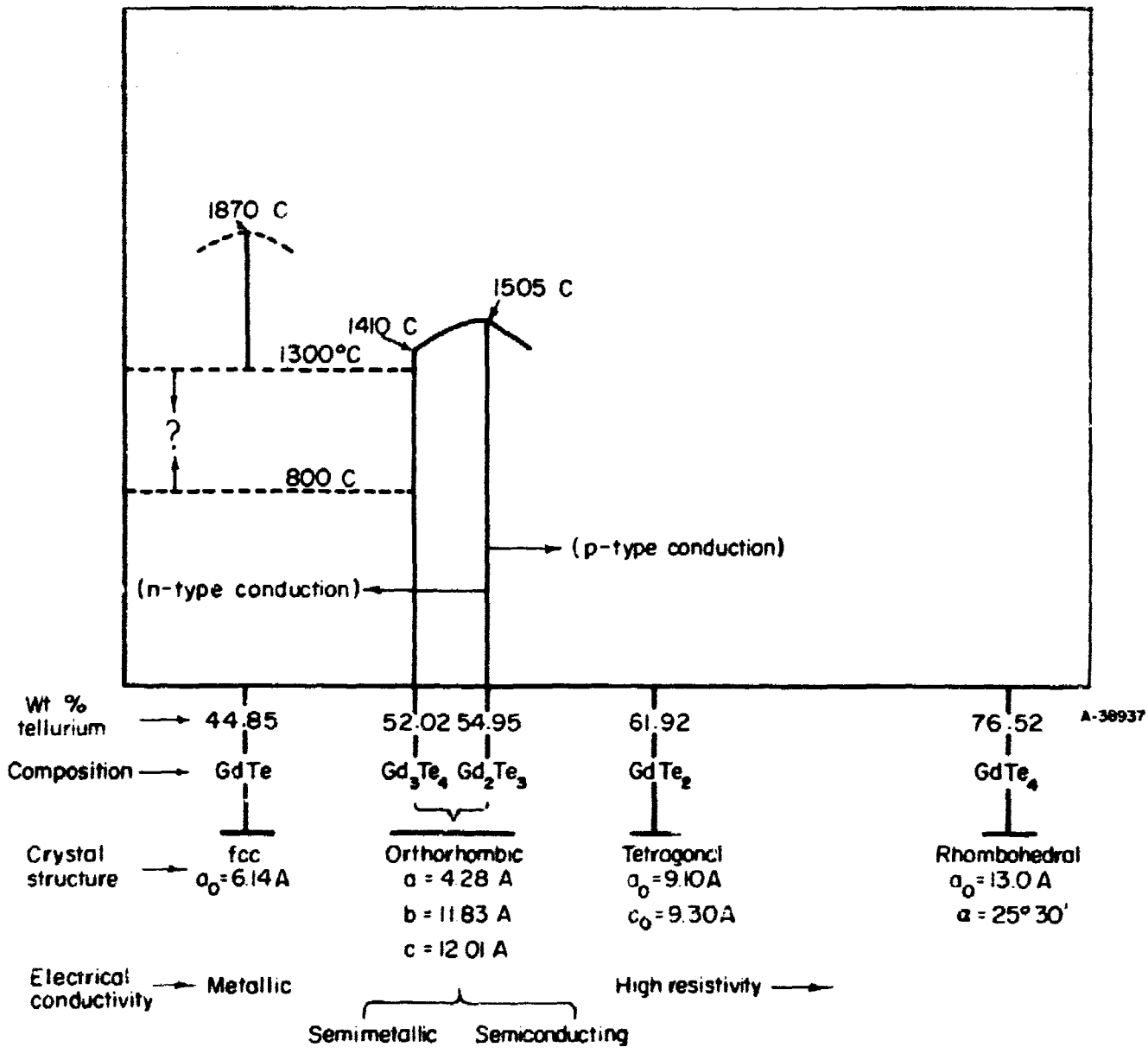

FIGURE 4. DATA FOR THE Gd-Te SYSTEM

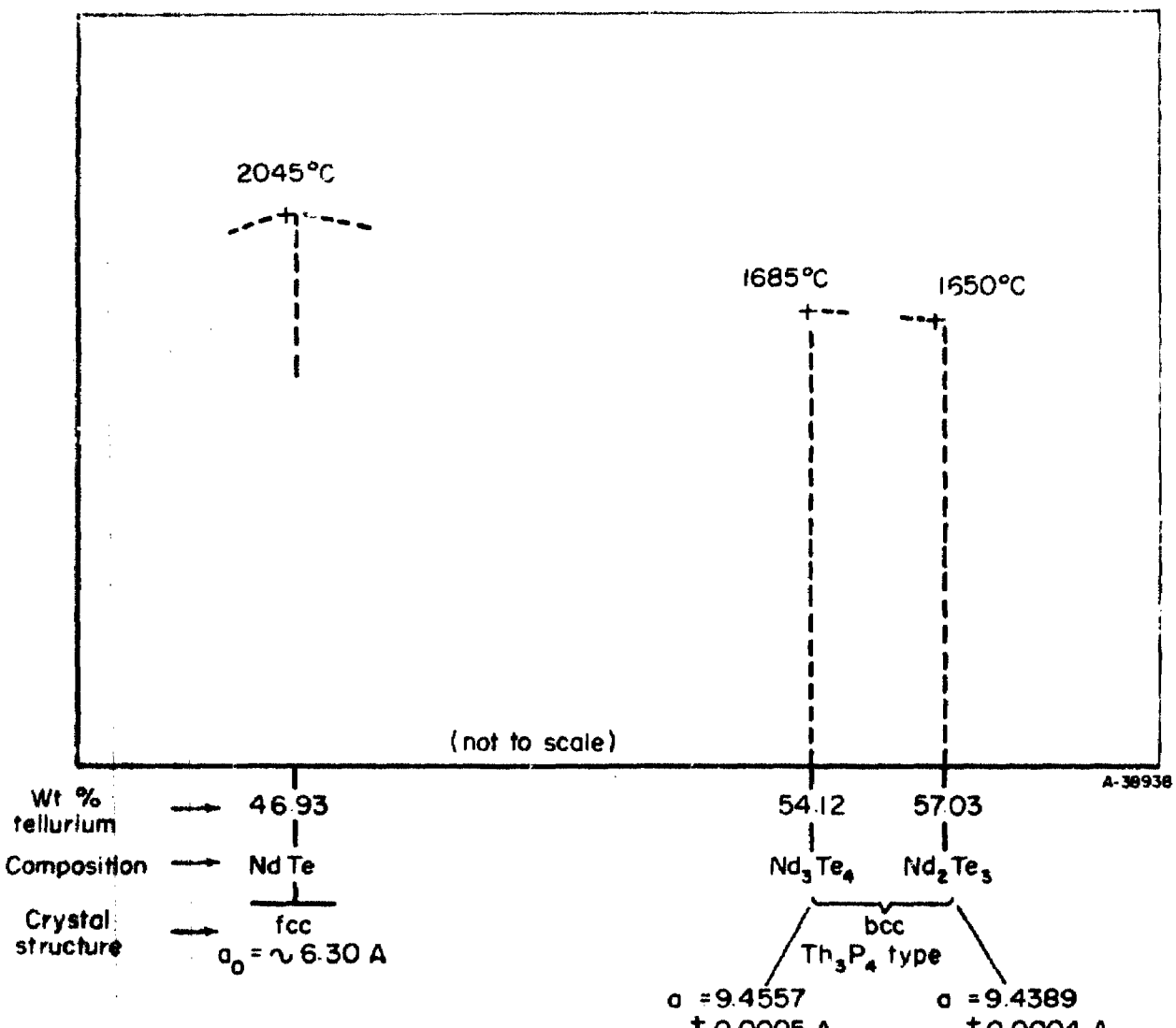

FIGURE 5. DATA FOR THE Nd-Te SYSTEM

In all systems studied in this research, the monoselenide or monotelluride appeared to be the highest-melting phase in the system. The data on the Gd-Te system (Figure 4) indicate that a phase boundary, extending from Gd to Gd_3Te_4 may exist at a temperature between 800 and 1000 C; its exact location on the temperature scale has not been determined. However, it has been noted that if a powdered mixture of equiatomic proportions of gadolinium and tellurium is held at 800 C, two phases, gadolinium and the Gd_3Te_4 phase, are formed which persist even after several hundred hours at temperature. On the other hand, in less than 6 hours at 1300 C, reaction is complete and single-phase GdTe powder is obtained. It is believed that this type of behavior is general and that high-temperature treatment is necessary in the preparation of the rare-earth monoselenides and monotellurides.

Monoselenides and Monotellurides

The monoselenides and monotellurides (MX) crystallize in the face-centered cubic, NaCl-type structure with cell sizes as indicated in Figure 6. The open data points are from Reference 3. The relatively large unit cell sizes for the samarium and ytterbium compounds indicate that, in these compounds, the divalent ions of the rare-earth metals dominate. A similar situation would be expected for the europium compound, since europium also exhibits a high stability in the +2 state, while the smaller cell parameters for NdTe, GdSe, and GdTe suggest that the rare-earth elements are present essentially as the +3 ion in these latter compounds.

In Figure 7, cell-size data, which are plotted for several sets of alloys of rare-earth monoselenides, show that cell size does not deviate significantly from Vegaard's law in the composition ranges studied. In the SmSe-NdSe system, in which both compounds exhibit n-type electrical conduction, the cell size is seen to change gradually from the high value for the samarium compound to the low value for the neodymium compound. In the YbSe-NdSe system the trend is seen to be similar; however, the effect of the lanthanide contraction in going from SmSe to YbSe also is apparent in the graphical data, and the range of cell sizes is much less in the latter system. (The electrical properties mentioned in this paragraph are discussed in greater detail in a subsequent section.)

M_3X_4-M_2X_3 Phases

The electrical properties most nearly resembling those of typical semiconductors were observed for compositions in the range M_3X_4-M_2X_3, where M is a rare-earth element which normally exhibits a tripositive oxidation state, and X is selenium or tellurium. Consequently, some study was made of these materials to develop some measure of understanding of the interrelation between their physical and chemical properties.

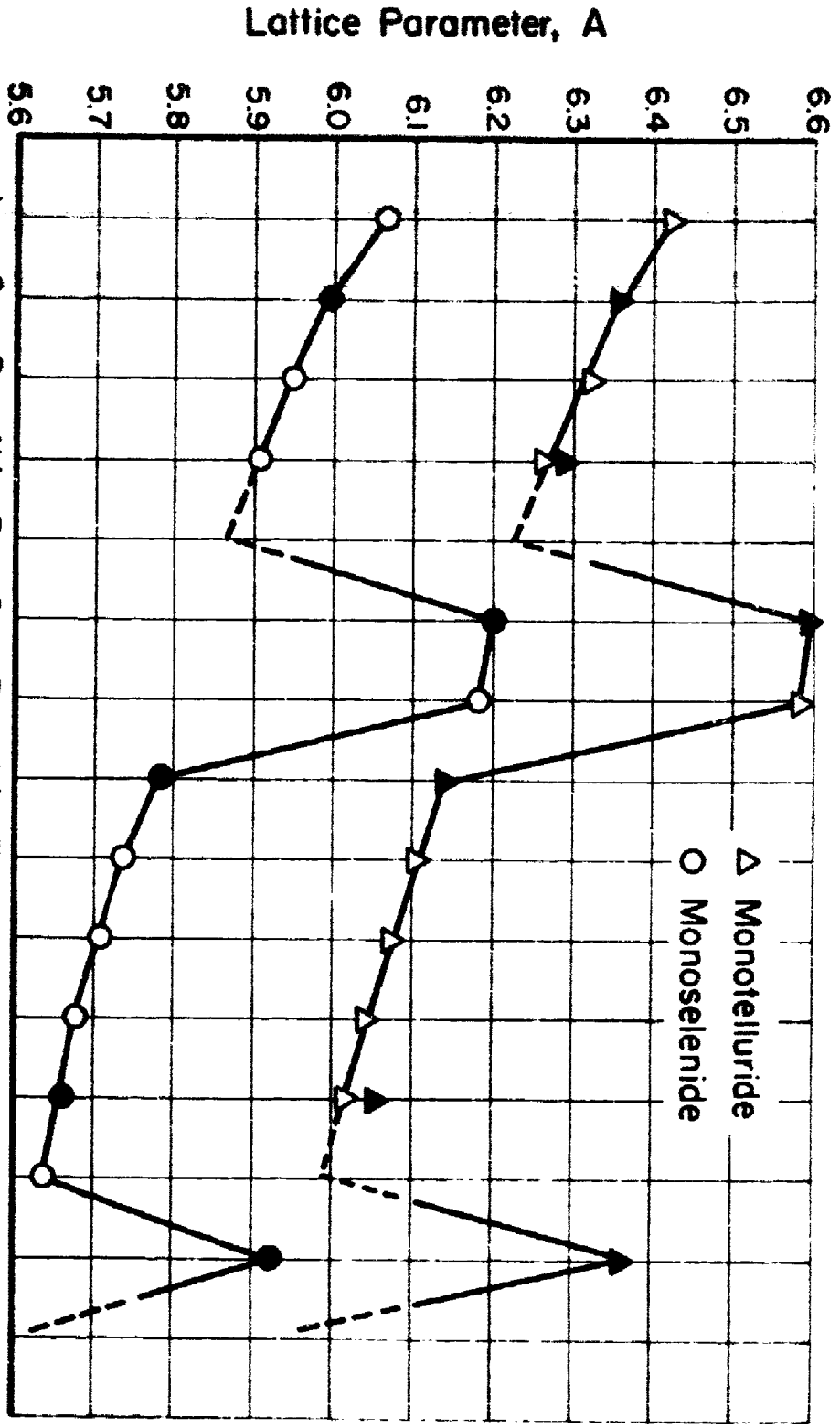

FIGURE 6. CELL SIZES FOR RARE-EARTH MONOTELLURIDES AND MONOSELENIDES

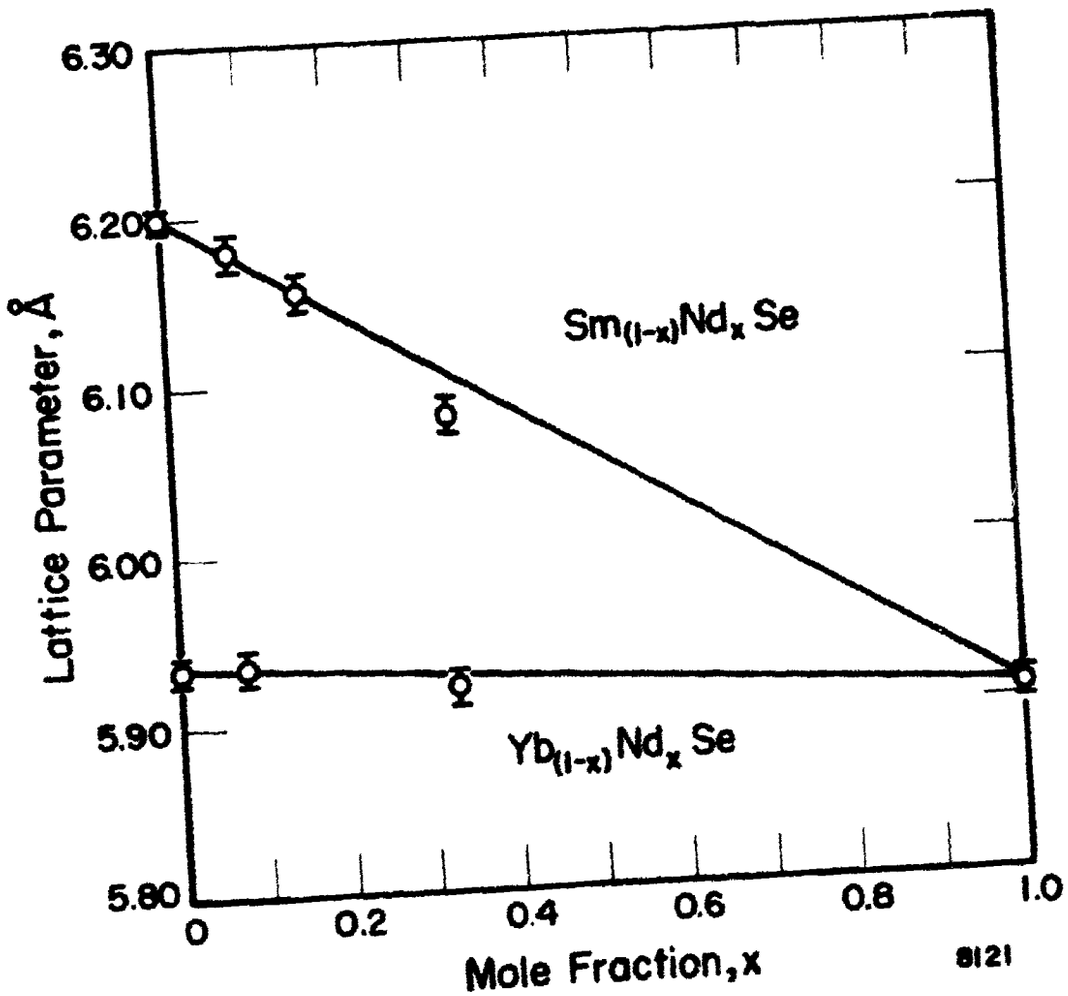

FIGURE 7. CELL SIZES FOR ALLOYS OF RARE-EARTH MONOSELENIDES

The Thorium Phosphide Structure

The body-centered cubic, Th_3P_4-type ($D7_3$) structure has usually been observed to prevail across the M_3X_4-M_2X_3 composition range in the subject systems in which M is a rare-earth element and X is sulfur, selenium, or tellurium. Available data on lattice constants for these compositions are presented in Table 6.

If it is assumed that all metal-metalloid bonds are equivalent in the crystals of the rare-earth compounds, metal-metalloid and metalloid-metalloid internuclear distances can be calculated from the lattice constants. These data are given in Table 7.

A first indication of the nature of the chemical bonding in the subject crystalline phases can be obtained by comparing the sums of the ionic and covalent radii of the appropriate elements with the observed internuclear spacings (Table 6). It is apparent from such a comparison that, even though some uncertainty may exist concerning the radius values and further uncertainty may result from the assumption of equivalent bonds (Ref. 9) the bonding must be neither purely ionic nor purely covalent. Specifically, it can be noted that the metal-plus-metalloid radius sums are less than the observed internuclear distances in all compositions for both the ionic and covalent cases. It is probable then that the cell sizes are determined by the anion-anion internuclear distances. From the radius data for the metalloids it appears that, if the bonding were purely covalent, the cell dimensions would be smaller than observed. On the other hand, if the bonding were purely ionic, the unit cells would be larger than observed, as can be seen from the data given. One is then led to the conclusion that the chemical bonding in the materials is partially ionic and partially covalent in character. Previously reported (Refs. 5, 9, 10) observations on structures of individual compounds in these systems and on transport properties are consistent with this conclusion.

An estimate of the covalent contribution to the bonding can be obtained in the following way. It is assumed that (1) anion-anion contacts prevail in the crystals, (2) all metal-metalloid bonds are equivalent, and (3) the degree of covalent (or ionic) character of the bond varies linearly with the apparent radius of the metalloid between the ionic and covalent values. The apparent radius of the metalloid element in the crystal is then just half of the metalloid-metalloid internuclear distance calculated from the cell constant. The covalent contribution to the bonding can be calculated from the apparent radius values, which are given in Table 7, by utilizing the relationship:

$$\% \text{ cov} = \frac{(r_{X\ ion} - r_{X\ app}) \times 100}{r_{X\ ion} - r_{X\ cov}},$$

in which $r_{X\ ion}$, $r_{X\ cov}$, and $r_{X\ app}$ are the ionic, covalent, and apparent metalloid radii, respectively. The absolute values of the covalent contributions, so obtained, will depend upon the radius values used. Since the tetrahedral covalent radii of the metalloid elements were employed, the estimates of the covalent contributions given here (Table 7) are thought to represent lower limits. It is probable that the octahedral covalent radii of the metalloids (which must be considered since CN = 6 for the metalloid elements in the Th_3P_4-type structure) will be somewhat greater than the tetrahedral radii for the respective elements. For example, in selenium it is likely that the 4d orbitals may be utilized in the octahedral (covalent) bonds, thus increasing apparent radius of the metalloid. It has, in fact, been noted (Ref. 8) that the octahedral radii of Se^{IV} and Te^{IV} are ~23 per cent greater than the tetrahedral radii of the respective elements. (Ref. 8).

TABLE 6. CRYSTAL-STRUCTURE DATA ON M_3X_4, M_2X_3 COMPOSITIONS

(BCC, D^3_3, Th_3P_4 Type)

Composition	a_0, A	Reference[a]	M-X Distance, A: Observed (0.346 a_0)	M-X Distance, A: Calculated $r_M + r_X$[b] Ionic	M-X Distance, A: Calculated $r_M + r_X$[b] Covalent	X-X Distance, A: Observed (0.375 a_0)	X-X Distance, A: Calculated $2r_X$[b]		
									Covalent
La_3S_4	8.730	3	3.021	2.90	2.73	3.274	3.68		2.08
Ce_3S_4	8.625	3	2.985	2.87	2.69	3.234			
Pr_3S_4	8.591	3	2.973	2.85	2.69	3.222			
Nd_3S_4	8.524	3	2.950	2.84	2.68	3.196			
Sm_3S_4	8.556	3	2.961	2.80	2.70	3.209			
Eu_3S_4	8.537	3	2.954	2.79	2.89	3.202			
La_2S_3	8.727	3	3.019	2.90	2.73	3.272			
Ce_2S_3	8.630	3	2.986	2.87	2.69	3.236			
Pr_2S_3	8.593	3	2.974	2.85	2.69	3.222			
Nd_2S_3	8.527	3	2.951	2.84	2.68	3.197			
Sm_2S_3	8.448	3	2.923	2.80	2.70	3.167			
Eu_2S_3	8.415	3	2.912	2.79	2.89	3.156			
Gd_2S_3	8.357	3	2.902	2.78	2.65	3.145			
Dy_2S_3	8.242	3	2.869	2.75	2.63	3.110			
La_3Se_4	9.055	3	3.135	3.04	2.83	3.395	3.96		2.28
Ce_3Se_4	8.973	3	3.104	3.01	2.79	3.386			
Pr_3Se_4	8.927	3	3.089	2.99	2.79	3.348			
Nd_3Se_4	8.853	3	3.065	2.98	2.78	3.322			
Sm_3Se_4	8.84	3	3.06	2.94	2.80	3.32			
Gd_3Se_4	8.718		3.024	2.92	2.75	3.269			
La_2Se_3	9.05		3.13	3.04	2.83	3.39			
Ce_2Se_3	8.96		3.10	3.01	2.79	3.36			
Nd_2Se_3	8.85		3.06	2.98	2.78	3.32			
Sm_2Se_3	8.785	3	3.040	2.94	2.80	3.294			
Gd_2Se_3	8.72	4	3.02	2.92	2.75	3.27			
Ce_3Te_4	9.566	3	3.303	3.24	2.97	3.587	4.42		2.64
Nd_3Te_4	9.4557		3.272	3.21	2.96	3.546			
La_2Te_3	9.62		3.33	3.27	3.01	3.61			
Ce_2Te_3	9.55		3.30	3.24	2.97	3.58			
Nd_2Te_3	9.4389		3.266	3.21	2.96	3.539			
Sm_2Te_3	9.48[c]		3.28	3.17	2.98	3.56			

(a) Nonreferenced values are from this work.

(b) Radii taken from various sources: r_M ionic (Ref. 6); r_M and r_X covalent (Ref. 7); r_X ionic (Ref. 8).

(c) Specimen contained a minor second, fcc phase.

TABLE 7. CALCULATED COVALENT CHARACTER OF BONDING

Composition	Apparent r_X, A	Calculated Per Cent Covalent Bond Character[a]	Composition	Apparent r_X, A	Calculated Per Cent Covalent Bond Character[a]
La_3S_4	1.637	25	La_2Se_3	1.70	33
Ce_3S_4	1.617	27.5	Ce_2Se_3	1.68	35.8
Pr_3S_4	1.611	28.8	Nd_2Se_3	1.66	38
Nd_3S_4	1.598	30	Sm_2Se_3	1.647	39
Sm_3S_4	1.604	30	Gd_2Se_3	1.64	40.5
Eu_3S_4	1.601	30			
			Ce_3Te_4	1.744	47.2
La_2S_3	1.636	25	Nd_3Te_4	1.773	49.5
Ce_2S_3	1.618	27.5			
Pr_2S_3	1.612	28.6	La_2Te_3	1.80	46
Nd_2S_3	1.598	30	Ce_2Te_3	1.79	47
Sm_2S_3	1.584	32.5	Nd_2Te_3	1.770	49.5
Eu_2S_3	1.578	32.5	Sm_2Te_3[b]	1.78	48
Gd_2S_3	1.572	33.8			
Dy_2S_3	1.555	35			
La_3Se_4	1.698	33			
Ce_3Se_4	1.693	34.6			
Pr_3Se_4	1.674	37			
Nd_3Se_4	1.661	38			
Sm_3Se_4	1.66	38			
Gd_3Se_4	1.634	41.7			

(a) $\%\ \text{cov} = \dfrac{(r_{X\ \text{ion}} - r_{X\ \text{app}}) \times 100}{r_{X\ \text{ion}} - r_{X\ \text{cov}}}$.

(b) Two-phase specimen.

Although the absolute values of the covalent contributions will depend upon the radius values used, the relative magnitudes will not. Hence, analysis of trends in the results should be valid. The calculated values of the degree of covalent bond character (Table 7) show, in general, the expected trends. The covalent contribution is least in the sulfides, intermediate in the selenides, and greatest in the tellurides. Also, within a given series, as the rare-earth component trends toward decrease in size (e.g., in going from La_2S_3-Dy_2S_3), the calculated covalent contribution increases, as might be expected from consideration of other general principles which apply.

No difference between values, and trends in the values, for the two compositions (M_3X_4 and M_2X_3) is apparent in the tabulated values of the covalent contribution. However, a plot of the fraction of covalent bond character against atomic number (Figure 8) reveals that, while the curves for the M_3X_4 sulfides and selenides do not deviate seriously from a monotonic increase, the curves for the M_3X_4 compositions tend to level off for samarium and europium. The degree of covalent character in the bonding of the compounds or compositions containing these elements may remain low because of the tendency of these rare-earth elements (samarium and europium) to achieve the spectroscopically stable $4f^7$ electronic configuration (Ref. 11), and thus to hold closely electrons which might otherwise contribute to covalent bonding.

Relationship of Structure to Electrical Properties

The observations regarding the nature of the chemical bonding in these rare-earth sulfide, selenide, and telluride phases (Th_3P_4 type) also are, in general, consistent with observed electrical properties of the materials. Observed carrier mobilities for the Th_3P_4 phases of the sulfides and selenides have been very small – of the order of magnitude of those expected for solids in which highly polar bonding prevails. It has, in fact, been suggested that electrical conduction in the sulfides can be characterized in terms of a hopping mechanism (Ref. 10) or a polaron model (Ref. 12), both of which imply localized charges. On the other hand, appreciable carrier mobilities, suggesting similarity to the covalently bonded broad-band semiconductors, have been observed for certain of the rare-earth tellurides which, although falling within the subject composition range, exhibit a somewhat different structure. Highest observed carrier mobilities have been for Gd_2Te_3, for which the covalent contribution to the bonding, as calculated, would seem to be approaching 50 per cent. In addition, Battelle has, in its laboratories, been able to prepare both n- and p-type specimens (single-phase material) of only Nd_2Te_3 and Gd_2Te_3 in the subject class of compositions.

The Gadolinium Telluride Structure

Along with the observed change in character of the electrical properties, a change in crystal-structure type also has been noted. As is illustrated in Figure 9, the Th_3P_4-type structure has not been obtained in specimens of Gd_2Te_3, Gd_3Te_4, or these (3-4 and 2-3) selenides and tellurides of the listed rare-earth elements beyond gadolinium in the series. The method of preparation, which has been described previously, was similar in all cases (with the exception, as noted below, of that employed for Dy_2Se_3). Quenching in air from temperatures near the melting points was involved, thus making it unlikely that the transformation to a low-temperature phase occurred.

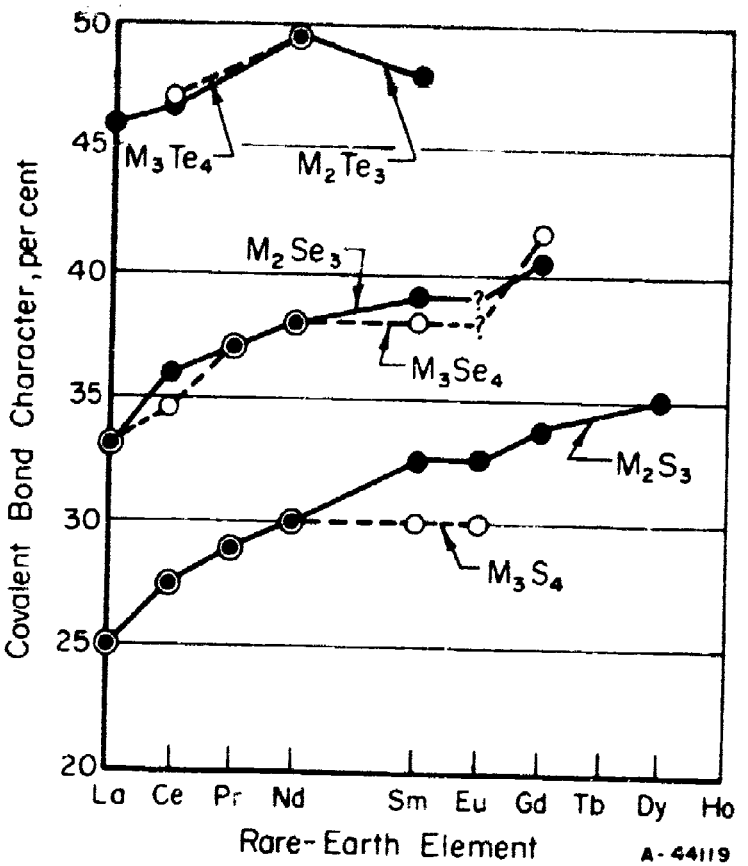

FIGURE 8. CALCULATED COVALENT CHARACTER OF BONDING IN RARE-EARTH SULFIDES, SELENIDES, AND TELLURIDES

La_2Se_3 Th_3P_4	Ce_2Se_3 Th_3P_4	Nd_2Se_3 Th_3P_4		Gd_2Se_3 Th_3P_4	Dy_2Se_3 Orthorh. a = 3.69 A b = 10.85 A c = 11.0 A	Er_2Se_3 Two phase, one fcc (ErSe)	Yb_2Se_3 Two phase, one fcc (YbSe)
La_2Te_3 Th_3P_4	Ce_2Te_3 Th_3P_4	Nd_2Te_3 Th_3P_4 >1000 C (orthorh.) similar to Gd_2Te_3 <1000 C	Sm_2Te_3 Th_3P_4 plus minor fcc phase (SmTe)	Gd_2Te_3 Orthorh. a = 4.28 A b = 11.83 A c = 12.01 A		Er_2Te_3 Two phase, one fcc (ErTe)	Yb_2Te_3 Two phase, one fcc (YbTe)

A-44120

FIGURE 9. CRYSTAL STRUCTURES TYPICALLY OBSERVED IN RARE-EARTH SESQUISELENIDE AND SESQUITELLURIDE SPECIMENS

In addition, a large number of specimens of Gd_2Te_3 and Gd_3Te_4 have been prepared, and all have displayed the orthorhombic structure. This structure was indexed from patterns obtained on single crystals grown by vapor deposition. It appears to be related to the tetragonal structure, tentatively reported previously (Ref. 1), through a slight displacement of atoms and a transformation of axis; unit cell volumes are the same. The composition limits of the structure appear to be near the Gd_2Te_3 composition on the tellurium-rich side. Specimens from Gd_3Te_4 synthetic compositions occasionally were observed to contain traces of the fcc GdTe phase, while those from Gd_2Te_3 synthetic compositions often contained traces of the tetragonal $GdTe_2$ phase. In the latter case, indications of the onset of p-type electrical conduction accompanied appearance of the second $GdTe_2$ phase. However, single-phase (orthorhombic) p-type specimens were obtained, and it is therefore concluded that the limit of stability of the Gd_2Te_3 phase is probably at slightly higher tellurium concentrations – i.e., slight concentrations of excess tellurium can be dissolved in the solid orthorhombic phase.

A structure similar to that of gadolinium telluride was obtained in Nd_2Te_3 by heat treating specimens in vacuo for 2 hours at 1000 C. Although the cell parameters have not been determined accurately, the X-ray diffraction patterns indicate that the structure is orthorhombic, with the cell being slightly larger than that for Gd_2Te_3. As is shown in Figure 9, an orthorhombic structure has also been observed for D_2Se_3. However, the possibility that this is a low-temperature phase cannot be ruled out in this instance, since the single-crystal specimen was prepared by use of a chemical reaction at 900 C. The tendency for specimens of the erbium and ytterbium compounds to be polyphase also strongly suggests that the Th_3P_4-type structure may not be stable in the selenides and tellurides of heavier rare-earth elements.

The Crystal-Structure Transition

The apparent limit of stability of the Th_3P_4-type structure cannot be explained on the basis of limits of stability for the packing (i.e., a radius-ratio limit). As has been shown, metalloid-metalloid contacts probably prevail throughout the series of compositions. Therefore, the changing cell size within a given series indicates that consideration of the packing of fixed-size "hard-sphere" anions does not apply. The radius ratios normally apply only if the materials are predominantly ionic. They were, nevertheless, calculated for the subject compositions, utilizing ionic, covalent, and apparent radii. The results show no trends toward pertinent limits of stability of the coordination polyhedra in any of the cases. On the other hand, it is seen from the analysis presented of the nature of the chemical bonding in the materials that an appreciable degree of covalent character might be expected in the bonding in selenides and tellurides of rare-earth elements near the end of the series. It is hypothesized that the observed change in crystal structure is brought about by the increasing degree of covalency of the bonding which, due to the directional character of the covalent bonding orbitals, calls for a change in coordination.

From first examination it would appear that the coordination which prevails in the Th_3P_4-type structure could also prevail in situations which call for predominantly covalent bonding. Stable arrangements might be the sp^3d^2 configuration for the octahedral bond orbitals of the metalloid, and a suggested $5p^35d^46s^1$ configuration for the required dodecahedral rare-earth orbitals. However, X-ray diffraction data indicate an approximately 25 per cent increase in density in going from the Th_3P_4 to the

orthorhombic structure. This suggests that the dodecahedral arrangement of the metalloid nuclei around the rare earth (in which the rare earth is an oversized "cage") no longer prevails, but may be replaced by an arrangement in which metal-metalloid coordination is lower. Evaluation of the hypothesis does not appear to be possible with information available at the present time. Additional data on the specific crystal structures involved and comprehensive examination of possible covalent bonding configurations will be required.

Alloys

Crystal-structure data were obtained also on some alloys which crystallized in the Th_3P_4-type structure. Data for the alloys in which SrSe was substituted for CeSe in the base composition, Ce_3Se_4, are shown in Table 8. As can be noted, the structure remains Th_3P_4-type through the alloy composition range studied, and the unit-cell size increases slightly as the SrSe concentration increases. The change is slight, however, and the trend is consistent with the data presented in the preceding discussion, which shows a gradual increase in cell size as size of the species of the metallic element present is increased.

TABLE 8. CRYSTAL-STRUCTURE DATA ON $Sr_xCe_{3-x}Se_4$ ALLOYS

Synthetic Composition	Crystal Structure	Lattice Parameter, a_o, A
Ce_3Se_4	Bcc, Th_3P_4 type	8.973
$Sr_{0.35}Ce_{2.65}Se_4$	Ditto	8.98
$Sr_{0.75}Ce_{2.25}Se_4$	"	9.0404
$SrCe_2Se_4$	"	9.0998

Other Selenides and Tellurides

As is indicated in Figures 4 and 5, compounds containing higher concentrations of the metalloid tend to crystallize in structures of lower symmetry. The $GdTe_2$ structure, for example, is tetragonal, with a = 9.10 A, c = 9.30 A. The structure apparently contains 8 formula units per unit cell; density calculated from X-ray data on this basis was 6.8 g/cm^3, which agrees well with the roughly measured density of 6.7.

$CeSe_2$, which was prepared by melting and casting material with composition near $CeSe_2$ in an atmosphere of selenium vapor, was found to have a tetragonal structure with a_o = 8.40, c/a = 1.005. The $CeSe_2$ differed somewhat from the $GdTe_2$, and other tetragonal structures reported for rare-earth selenides and tellurides, with respect to the atom arrangements.

PURITY OF STARTING MATERIALS

In general, the standard grades of rare-earth metals readily available from commercial sources were utilized. In several cases, however, some further purification of the metals was accomplished.

As can be seen in Table 9, where data on suppliers' typical analyses and analyses of the specific lots of metals utilized are tabulated, purity of the standard grade of rare-earth metals is low (99+%), relative to the usual standards for electronic materials. In metals as reactive as the rare earths, one might tend to be concerned first about the concentrations of oxygen and other gaseous impurities. It can be noted that oxygen concentrations are, indeed, high. However, the concentrations of several of the metallic impurities (e.g., tantalum, calcium, iron, and copper) are of comparable magnitude, indicating that the importance of oxygen as an impurity in the compounds may not surpass that of any one of several metallic elements.

As is shown in the first three entries in Table 10, significant purification of samarium metal was achieved by vacuum distilling the metal and condensing the product at a temperature below its melting point (work done in the course of this project). Concentrations of the metallic impurities calcium, magnesium, and molybdenum were sharply reduced by the process. However, no difference was detected between the electrical properties of SmAs prepared from the as-received metal, and those of SmAs prepared from the purified metal. On the other hand, differences were noted between the electrical properties of Nd_2Te_3 specimens prepared from different lots of neodymium metal: Nd-I and Nd-II (see Table 10). The specimens prepared from Nd-I metal were consistently p-type, presumably because of the calcium and/or tantalum present, whereas the specimens containing Nd-II metal were consistently n-type.

The selenium, tellurium, arsenic, and antimony used to synthesize the compounds were of higher purity (at least 99.99+%) than the rare-earth metals. The contribution of charge carriers from these sources is, therefore, believed to be negligible with respect to (1) those from impurities present in the rare-earth elements, (2) those from impurities introduced in the course of synthesis of the compounds, and (3) those arising as results of deviations from stoichiometry.

ELECTRICAL PROPERTIES

Electrical measurements were made on specimens cut or cleaved from the various ingots. Parallelepipeds were shaped by lapping the specimens with 600-grit SiC paper. Both the cutting and lapping were done in a dry state since the compounds, in general, tend to hydrolyze. Ohmic contacts were made by applying indium solder with an ultrasonic tool.

The apparatus used for high-temperature (to 1300 K) resistivity and Seebeck coefficient measurements utilized spring-loaded pressure contacts. The specimens were held between platinum end plates which served as sample-current contacts. Platinum-platinum 10 per cent rhodium thermocouples, or Chromel-Alumel

TABLE 9. TYPICAL ANALYSES OF RARE-EARTH METALS[a]

Impurity Element	Impurity Concentrations, ppm, in Indicated Metal					
	Ce	Nd	Sm	Gd	Er	Yb
Ta	~1000	800-1000	100-1000	~300	~2200	~1000
Ca	200-500	200-500	100-1000	~100	1000-2000	100-1000
Mg	300-1000	~100	10-10,000	--	--	~100
Fe	300-3000	200-500	~300	~1000	--	~300
Ni	--	~100	~200	~1000	~1000	400-1000
Cu	--	~2000	~100	~100	--	10
Al	--	~500	~100	--	--	--
Si	--	~100	~100	~100	--	--
Other rare-earth elements	~1000	~250	200-1000	~700	~2000(Tm)	~1000
O_2	500-2000	1000-2000	500-2500	1000-2800	~1200	--
N_2	50	--	--	20	--	--
Total	3350-8500	5250-7050	1700-6400[b]	4300-6100	7400-8400	2900-4400

(a) Results derived from suppliers' typical analyses and analyses of specific lots utilized are given. Ranges of impurity concentrations given reflect variation of values from sample to sample, lot to lot, and supplier to supplier for the subject metal.

(b) Excluding magnesium.

TABLE 10. RESULTS OF SPECTROGRAPHIC ANALYSES OF SELECTED SPECIMENS OF RARE-EARTH METALS

Material	Impurity Elements Detected, ppm by weight											Total Detected
	Ca	Mg	Si	Ni	Fe	Mn	Cu	Al	O_2	Mo	Ta	
Sm, as received	500	~10,000	5	--	5	20	10	<10	--	2000	~10^4	~12,000[a]
Sm, distilled, condensed as liquid	10	5	10	--	10	50	100	<10	--	20	<10^5	205[a]
Sm, redistilled, condensed as solid	10	10	10	--	20	10	50	10	--	10	<10^4	130[a]
Gd-I	300	--	--	--	500	--	--	--	1000	--	800	2,600
Gd-II	ND	ND	--	--	500	--	--	--	1000	--	ND	1,500

a) Excluding tantalum.

thermocouples, were utilized as current leads and to determine temperatures at the ends of the specimens. Point contacts of platinum or Chromel were pressed against a face of the specimen for resistivity-voltage measurements. All high-temperature electrical measurements were made in vacuum at residual pressures in the range 1×10^{-5} to 1×10^{-4} mm of Hg. This was found to be necessary in an early stage of the study of the selenides and tellurides. At pressures (or air) greater than 10^{-4} mm of Hg, irreversible changes in electrical properties of specimens, presumably resulting from oxidation of the materials, were observed to occur. At pressures less than $\sim 10^{-4}$ mm of Hg, reproducible results were obtained.

Monoselenides and Monotellurides

The rare-earth monoselenides and monotellurides form a family of refractory materials with interesting and potentially useful electrical properties. These compounds all crystallize in a fcc NaCl structure and have melting points in the range 1700 to 2100 C. Table 11 shows the room-temperature resistivity of some of the monoselenides and monotellurides which have been prepared.

TABLE 11. ELECTRICAL RESISTIVITY OF REPRESENTATIVE RARE-EARTH MONOSELENIDES AND MONOTELLURIDES

Synthetic Composition	Resistivity at 25 C, ohm-cm
SmSe	2000
SmTe	2000
YbSe	100
YbTe	7000
CeSe	1×10^{-4}
CeTe	2×10^{-4}
NdSe	5×10^{-5}
NdTe	4×10^{-5}
GdSe	8×10^{-5}
GdTe	7×10^{-4}
ErTe	1×10^{-4}

In terms of their electrical properties, these materials fall into two general classes: one class which will be referred to as Type II consists of compounds of rare-earth elements which normally exhibit a stable dipositive oxidation state, such as samarium and ytterbium; the other class which will be referred to as Type III includes compounds of rare-earth elements which normally exhibit a tripositive oxidation state, such as neodymium, gadolinium, and erbium. The Type II compounds exhibit relatively high resistivities, large negative temperature coefficients of resistance (negative TCR), and have low room-temperature free-carrier concentrations (10^{1} to

$10^{17}/cm^3$. The Type III compounds exhibit very low resistivities, positive TCR's, and appear to be degenerate semiconductors, or metallic in nature.

Figure 10 shows the temperature dependence of the electrical resistivity of various SmSe specimens. This material is characterized as n-type with room-temperature resistivity of about 2000 ohm-cm and carrier concentration of about $10^{15}/cm^3$. Although samples having resistivities which deviate from the more typical values in the low-temperature range can be prepared (e.g., Specimens 15B and 55 in Figure 10), the differences usually can be rationalized by pointing up obvious additions of impurities or defects (e.g., by deviation from stoichiometry) in substantial amounts. Single-crystal specimens exhibit electrical properties not materially different from those of polycrystalline specimens.

Hall data also indicate large temperature dependences suggesting a conduction mechanism involving the thermal activation of charge carriers. The fact that the high-temperature electrical properties are the same for so many samples prepared under a variety of conditions (e.g., with both purified and as-received samarium, with both excesses and deficiencies of samarium, and with additions of chemical impurities) suggests that the observed conductivity characteristics may be intrinsic to the material. Samarium in SmSe apparently shows a +2 oxidation state because the third normally available valence electron tends to reside in a 4f level in an attempt to achieve a stable half-filled $4f^7$ configuration (see Table I and Figure 6). Hence, the activation energy for conduction giving rise to $\rho \propto e^{0.36\ ev/kT}$ may be associated with an electron transition from a 4f level to a 5d or 6s conduction band. If classical semiconductor theory is applied, the forbidden energy gap, E_g, is calculated to be about 0.72 ev for SmSe, as determined from the limiting slope in Figure 10.

In contrast to the n-type SmSe, the monoselenides and monotellurides of ytterbium have exhibited hole conduction, presumably as a result of the presence of p-type impurities or lattice defects behaving as acceptor sites. Figure 11 shows the temperature dependence of resistivity for p-type YbSe and YbTe specimens. The two YbSe specimens have carrier concentrations on the order of $4 \times 10^{17}/cm^3$, with the hole mobilities being on the order of 0.3 cm^2/volt-sec. Activation energies of 0.17 ev and 0.3 ev can be calculated from the data ($\rho \propto e^{0.17/kT}$ and $\rho \propto e^{0.3/kT}$ in the range 300 to 500 K for YbSe Specimen 16B and YbTe Specimen 3, respectively, again assuming that classical semiconductor theory is applicable. At higher temperatures, the data indicate the possibility of approach to an intrinsic-conduction range; however, a slope is not well defined, and the specimen is still p-type at 1130 K (as determined from the sign of the thermoelectric power).

In the case of the Type III compounds, such as NdSe and the monotellurides of Nd, Gd, and Er, the above-described electron transition from a 4f level to a conducting state appears to occur readily at all temperatures above 4 K. It is noted that these rare-earth elements normally exhibit only the +3 oxidation state. In contrast with the Type II compounds, these Type III compounds exhibit low room-temperature resistivities, in the 10^{-5} to 10^{-4} ohm-cm range, and positive temperature coefficients of resistance, as is shown for GdTe in Figure 12. Also carrier concentrations in these materials, which are all n-type, are apparently very large; estimates of the concentrations fall in the range 10^{21} to $10^{22}/cm^3$. The source of these carriers is believed to be the excess valence electrons contributed by the 2×10^{22} rare-earth atoms per cm^3 in the lattice.

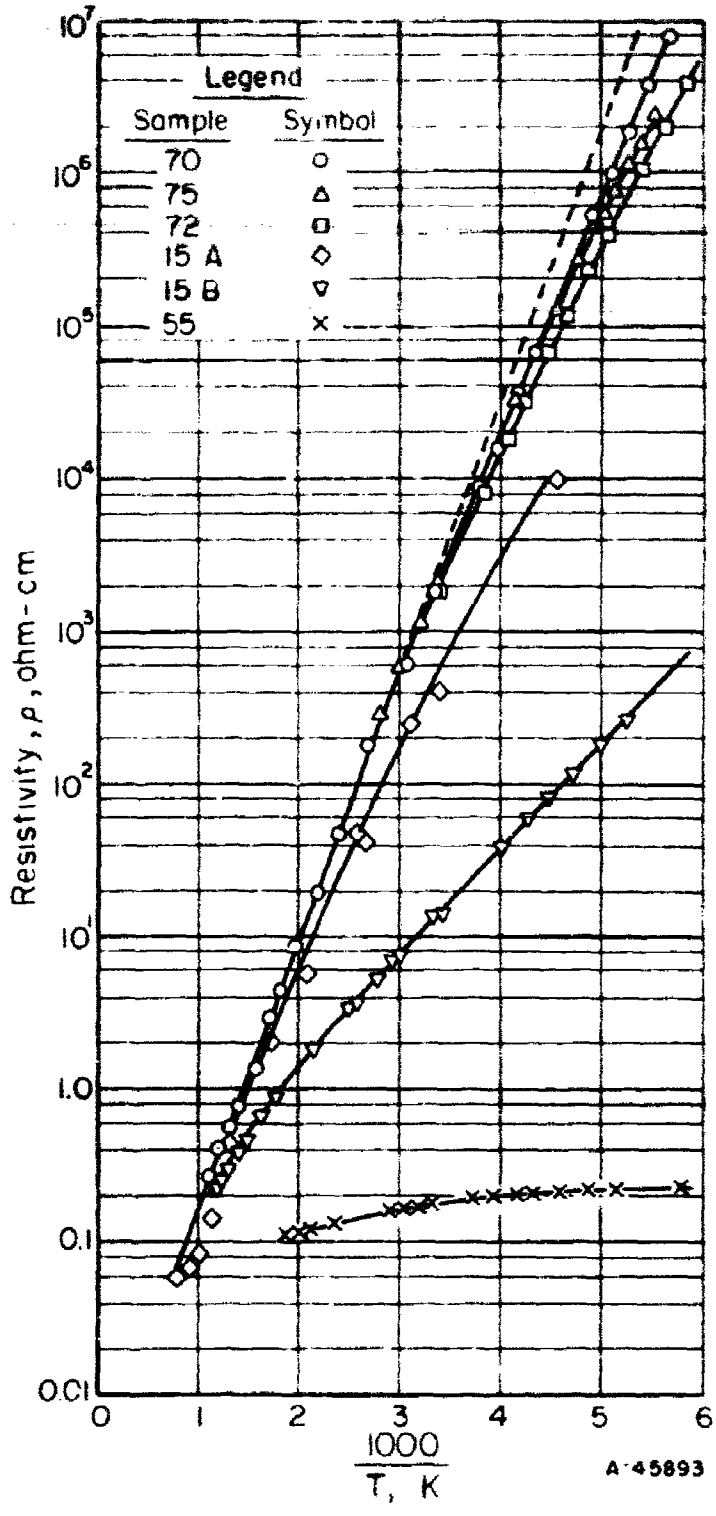

FIGURE 10. RESISTIVITY AS A FUNCTION OF TEMPERATURE FOR N-TYPE SmSe SAMPLES

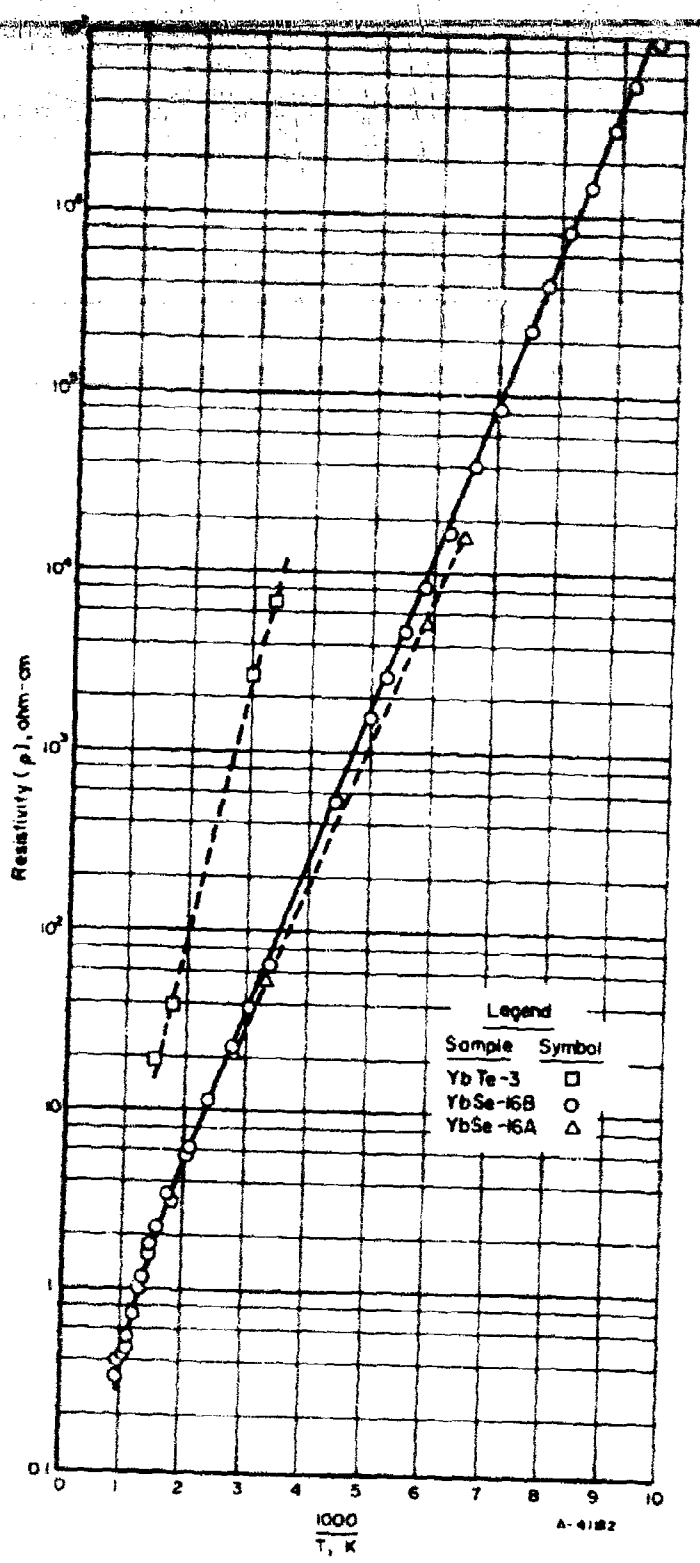

FIGURE 11. RESISTIVITY AS A FUNCTION OF TEMPERATURE FOR P-TYPE SPECIMENS OF YbTe AND YbSe

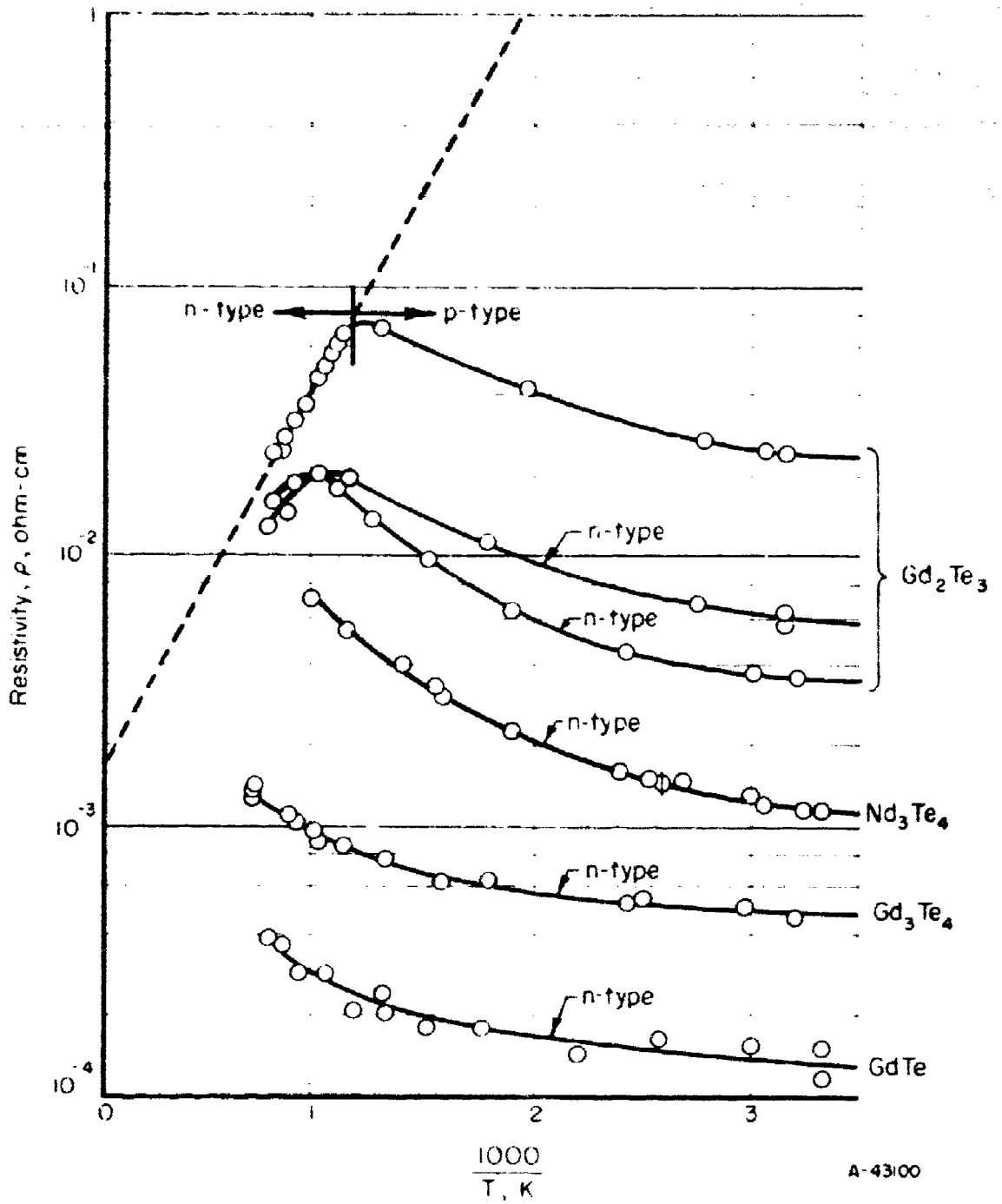

FIGURE 12. RESISTIVITY AS A FUNCTION OF TEMPERATURE FOR VARIOUS NOMINAL Gd-Te AND Nd-Te COMPOSITIONS

Alloys made up of a compound containing a dipositive metal ion, along with one containing a tripositive metal ion, have been prepared and are found to exhibit electrical properties intermediate between those of the two binary compounds. Figure 13, shows the Hall coefficient and resistivity of various compositions in the SmSe-NdSe alloy system. As samarium is replaced progressively with neodymium, the resistivity of the resulting compositions decreases from about 10^3 to 10^{-5} ohm-cm, with a precipitous drop of 4 orders of magnitude occurring within a narrow range at about 11 to 13 mole per cent NdSe. Carrier concentrations measured for alloys in the range 0 to 40 per cent NdSe also undergo an abrupt change at a composition containing about 12 mole per cent NdSe, suggesting that there are at least two distinct modes of conduction operating in the alloy system. The Hall coefficient value at 100 per cent NdSe is a calculated value based on the concentration of neodymium atoms, assuming one conduction electron per neodymium atom.

At low NdSe concentrations, one might expect each neodymium atom in the SmSe matrix to act as a donor impurity which is ionized at all temperatures. This is indeed not the case as illustrated by the following example. At concentrations of 2 mole per cent NdSe, approximately 4×10^{20} electrons/cm^3 should be seen if the neodymium atoms act as ionized donors. However, this alloy composition exhibits electrical properties essentially the same as those of pure SmSe, containing only about 10^{15} electrons/cm^3. In fact, at alloy compositions of 16 per cent NdSe (or about 3×10^{21} neodymium atoms/cm^3), only about 1.6×10^{20} electrons/cm^3 are found experimentally. In view of the very low electron mobilities observed for these materials, it would not be surprising to find that the mean free path for electrons is so small that standard band theory does not apply.

Electrical Conduction in the SmSe-NdSe Alloys

Consideration has been given to possible modes of electrical conduction in pseudobinary alloys of the SmSe-NdSe type. The nature, location, and cause of the abrupt change in electrical properties with composition (see Figure 13) were the initial subjects for analysis.

It should be recalled that, since samarium normally exhibits a highly stable dipositive oxidation state, in SmSe formal ionic valences are balanced ($Sm^{+2}Se^{-2}$) and low free-electron concentrations might be expected. On the other hand, neodymium normally exhibits only a tripositive oxidation state. Nevertheless, it is reasonable to expect that, in the compound NdSe, the bonding also will involve only two electrons, leaving one loosely held electron associated with each formula unit or each neodymium atom ($Nd^{+3}Se^{-2}+e^-$) which is free to act as a charge carrier. Thus it appears reasonable to consider the neodymium atoms a source of charge carriers and to expect a correlation between the carrier concentration and the concentration of neodymium atoms in the alloy.

The correlation between the two concentrations is not a direct one, however; the net carrier concentrations are observed to be very much smaller than the concentrations of neodymium atoms, as has been pointed out previously. In alloys containing less than approximately 11 mole per cent NdSe, the carrier concentrations are found to be less than 0.01 per cent of the neodymium-atom concentrations. For compositions containing

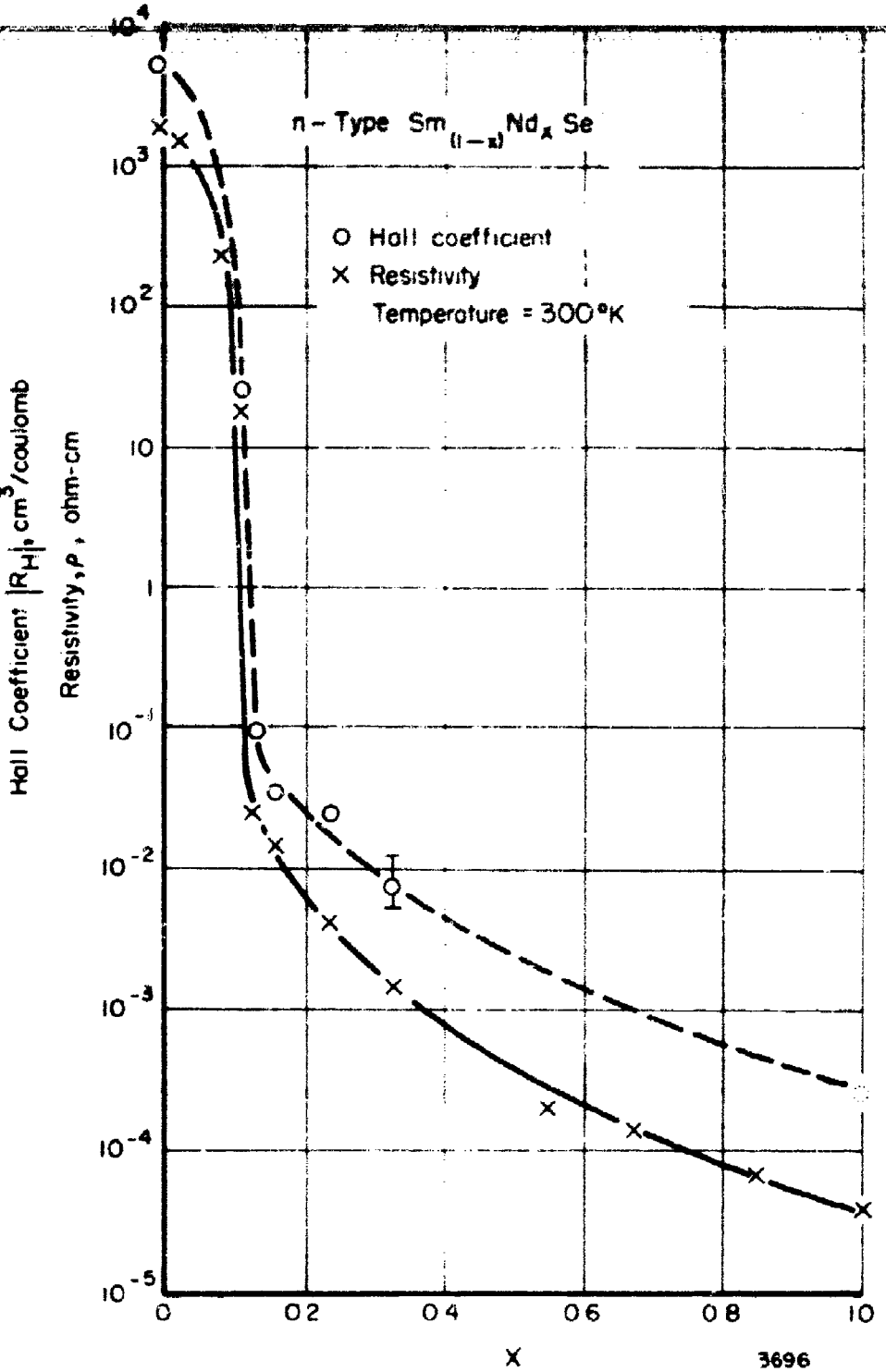

FIGURE 13. ELECTRICAL PROPERTIES OF COMPOSITIONS IN THE SmSe-NdSe ALLOY SYSTEM

more than about 13 per cent NdSe, the net carrier concentrations are only 3+ per cent of the neodymium-atom concentrations.

The following hypothesis was advanced and examined as a possible explanation for the abrupt changes in electrical properties. Electrical conduction is presumed to occur through interactions involving the third, loosely held, valence electrons of the neodymium atoms. It is further suggested that, above about 11 per cent NdSe, neodymium atoms which are close enough to interact can form chains of significant length; whereas, below about 11 per cent NdSe, the concentration of neodymium atoms in long chains becomes negligibly small compared to conduction electron concentrations associated with the SmSe matrix.

A rough statistical analysis was made to obtain an estimate of the concentration at which long chains of neodymium atoms on nearest-neighbor sites might begin to form. The essentials of the statistical analysis, the results of which appear to affirm the hypothesized involvement of nearest-neighbor interactions in the conduction process, are as follows. Consider a cube of material containing Nf neodymium atoms and N(1-f) samarium atoms (where f is the mole fraction of NdSe). The number of neodymium atoms on one face of the cube is $(Nf)^{2/3}$. If N is very large, the number, N_c, of chains of nearest-neighbor neodymium atoms beginning on this face of the cube and extending to the opposite face can be shown to be approximately:

$$N_c = (Nf)^{2/3} \prod_{p=0}^{\infty} \left[1 - (1-f)^{(n-1)\,\bar{m}^p} \right], \qquad (1)$$

where n is the number (12 in the NaCl structure) of cation nearest neighbors of a given cation and $\bar{m}$ is the average number of neodymium nearest neighbors of each neodymium atom. We assume $\bar{m}$ to be equal to nf, and we ignore any interlocking of chains or any "loop" formations. Equation (1) becomes

$$N_c/(Nf) = \prod_{p=0}^{\infty} \left[1 - (1-f)^{11(12f)p} \right] = \Psi(f) \qquad (2)$$

The function $\Psi(f)$ is zero for $12f < 1$ (i.e., for $\bar{m} \leq 1$), increases very rapidly as the composition is adjusted toward that at which $12f > 1$, and approaches 1 for $12f >> 1$. Thus this analysis predicts an abrupt, almost discontinuous rise in the concentration of neodymium atoms in long chains on nearest-neighbor cation sites at $f = 1/12 = 0.0833$. If interactions between such atoms are involved in electrical transport, a similar, rapid rise in conductivity would be predicted as the mole fraction of NdSe is increased through 8.3 per cent and values just above. The 8.3 per cent is, however, seen to be a lower limit because loop formations and the interlocking of chains have not been taken into account, and, in addition, no directional selection has been imposed. Also, the rise in conductivity would be expected to occur at a slightly higher concentration than that for the inception of chain formation.

The hypothesis was also evaluated by a second method. The statistical arrangements of atoms in alloys were investigated by randomly placing representative neodymium and samarium "atoms" into crystallographic models, varying both the alloy composition and the size of the model. The formation of chains or strings of neodymium atoms in nearest-neighbor sites was noted as the models were randomly filled.

Estimates of the concentrations of excess valence electrons which might be associated with such chains were made by assuming that one free (or loosely held) electron is associated with each neodymium atom.

It is not possible, with the present inadequate knowledge of band structure and energy levels in these compounds and alloys, to obtain corresponding conduction-electron concentrations from the estimates of excess valence-electron concentrations. However, it was found that some information could be gained about the conduction process by treating the data on atom arrangements in several ways and comparing the results with observed net free-carrier concentrations.

If it is assumed that the equivalent of one electron is contributed to the conduction process by each neodymium atom in the "conduction chains", then the calculated carrier concentrations (Curve A, Figure 14) are much higher than the experimentally measured values (open circles in the figure).

In a second way of examining the data, it is assumed that the excess valence electron initially associated with a neodymium atom is distributed such that the electron densities between the atom and all nearest-neighbor cations, regardless of identity, are the same. That is, on the average, the electron density between Nd-Nd nearest neighbors is equal to that between Nd-Sm nearest neighbors. Thus, for analytical purposes, the fraction of an excess valence electron considered to be occupying a given coordination leg in the cation sublattice changes with composition (i.e., as identity of the other 11 nearest neighbors of the atoms changes) as illustrated in Table 12. Note that at high "free" electron concentrations (f = 1), both neodymium and samarium show their lowest formal charges, as would be expected. With this assumed distribution, the concentration of excess valence electrons in Nd-Nd nearest-neighbor chains across the models shows the type of variation with changing alloy composition that conduction-electron concentrations would be expected to display.

TABLE 12. ASSUMED DISTRIBUTION OF VALENCE ELECTRONS IN CATION SUBLATTICE OF SmSe-NdSe ALLOY

Mole Fraction NdSe, f	Fraction of[a] Excess Valence Electron Associated With Nd-Nd or Nd-Sm Coordination Leg, λ	Formal[b] Charge on Nd, C_{Nd}	Formal[c] Charge on Sm, C_{Sm}
1	1/6	2	(1)
6/7	1/7	2+1/7	1+2/7
2/3	1/8	2+1/4	1+1/2
1/2	1/9	2+1/3	1+2/3
1/3	1/10	2+2/5	1+4/5
1/6	1/11	2+5/11	1+10/11
0	(1/12)	(2+1/2)	2

(a) $12f\left(\frac{\lambda}{2}\right) + 12(1-f)\lambda = 1$ or $\lambda = \frac{1}{12-6f}$

(b) $C_{Nd} = 2 + \frac{1}{2-f}$.

(c) $C_{Sm} = 2 - \frac{f}{2-f}$.

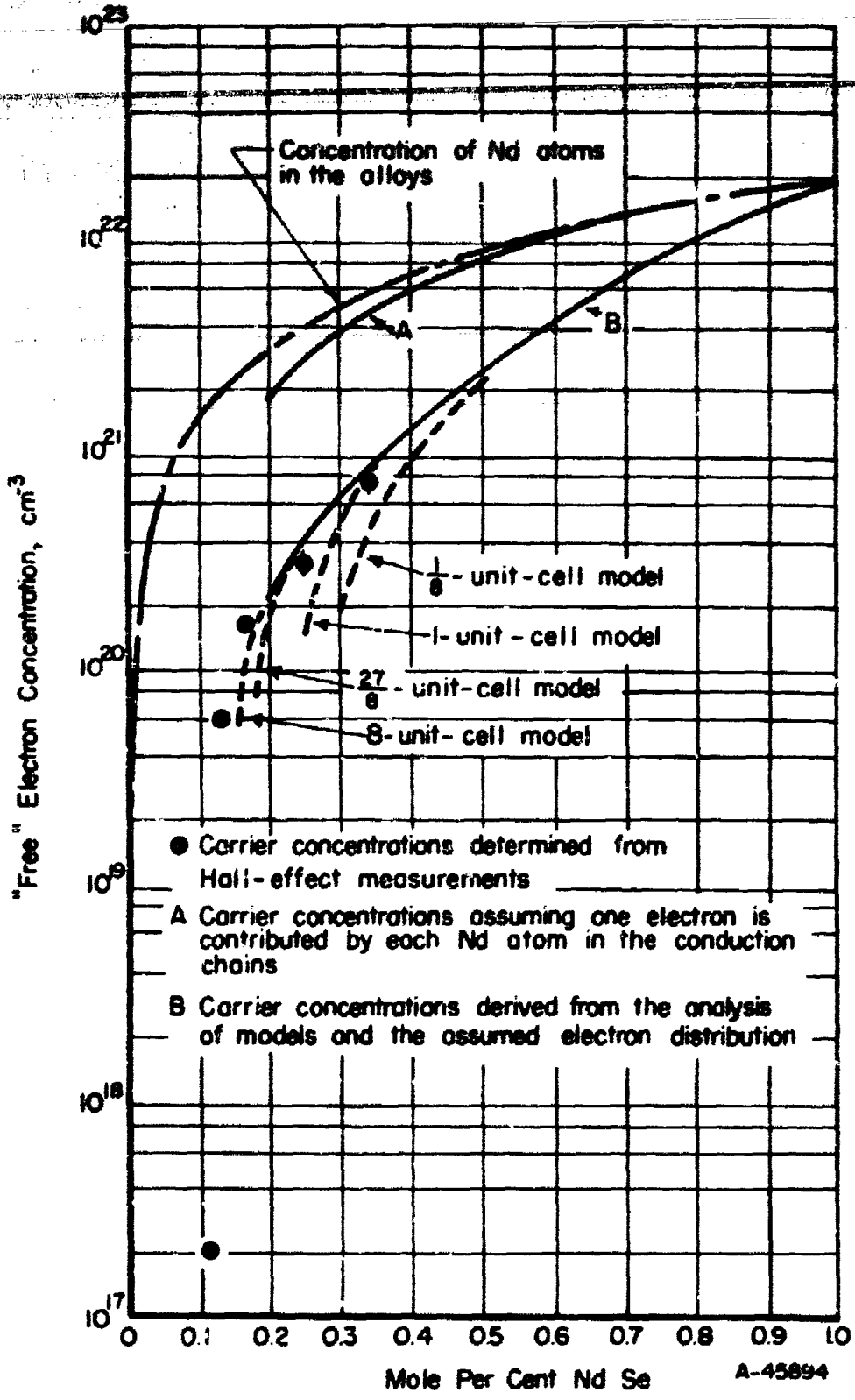

FIGURE 14. ELECTRON CONCENTRATIONS IN SmSe-NdSe ALLOYS

Further, if these electron concentrations are normalized with respect to the theoretical maximum electron concentration for pure NdSe*, the calculated values are in good agreement with the measured carrier concentrations, between 20 and 33 per cent NdSe, as can be seen in Figure 14. Curve B is a composite of data from analysis of the crystallographic models: a 1/8-unit-cell model over the range 50 to 100 per cent NdSe, a 1-unit-cell model over the range 31 to 100 per cent NdSe, a 27/8-unit-cell model for 32 to 54 per cent NdSe, and an 8-unit-cell model for the 19 to 31 per cent NdSe composition range. For each of the models, Curve B was extended down to somewhat lower NdSe concentrations (dashed branches) by use of the approximation:

$$C_2 \sim \frac{P_2}{P_1} \quad C_1 \ ,$$

where P_1 is the probability of finding a chain across a certain model at a known concentration C_1 and P_2 is the probability of getting a chain at a lower concentration C_2.

As can be seen, the carrier-concentration curves for the 1/8- and 1-unit-cell models fall off at higher NdSe concentrations than do those for the 27/8- and 8-unit-cell models. The trend indicates that if a much larger model were used, the abrupt change in predicted carrier concentrations would occur at a lower NdSe concentration, with the curve falling even nearer to the experimentally determined points.

Utilizing the crystal-model analysis, the effect of allowing next-nearest-neighbor interactions along with the nearest-neighbor interactions was investigated. The results do not agree with observed properties of the alloy specimens; predicted carrier concentrations are several orders of magnitude higher than experimentally determined concentrations.

Thus, the analyses indicate that, if the conduction process involves interactions between neodymium atoms in chainlike arrays on nearest-neighbor cation sites, an abrupt change in electrical properties would be expected to occur as the composition is varied between a lower limit of about 8.3 mole per cent NdSe, which is predicted by the approximate statistical analysis, and an upper limit of about 16 mole per cent NdSe, as determined by the crystal-model technique of analysis. This is in good agreement with experimental observations which place the break at about 12 per cent NdSe. In addition, as has been pointed out, both analytical techniques probably would predict transitions for compositions closer to experimental 12 per cent composition if the techniques were refined.

M_3X_4-M_2X_3 Selenides and Tellurides (Nd, Gd, and Ce)

Rare-earth selenide and telluride compositions ranging from M_2X_3 to M_3X_4, in which the rare-earth element is one normally exhibiting a stable +3 oxidation state, have been observed to have good thermal stability and to crystallize in either a bcc thorium phosphide structure or an orthorhombic structure. The lower atomic number rare-earth elements form phases which exhibit the Th_3P_4-type structure. For elements of higher atomic number than about 60 (neodymium), the tellurides assume the lower

*The theoretical value used was the concentration of neodymium atoms in pure NdSe. Thus it is assumed that one electron is contributed by each neodymium atom.

symmetry structure. The selenides of rare-earth elements heavier than gadolinium apparently crystallize in the orthorhombic structure. Details of observations on this subject are presented in the section on "Structure and Phase Relationships".

Figure 12 shows the temperature dependence of resistivity for Gd_2Te_3 and Gd_3Te_4 compositions which crystallize in the orthorhombic structure. For the 2-3 composition, both p- and n-type conduction are observed with carrier concentrations in the range 1×10^{19} to $6 \times 10^{19}/cm^3$. The top curve of Figure 12 is for a specimen which is p-type at low temperatures and crosses over to n-type at about 900 K. This sample was single-phase (the orthorhombic structure) material, which by chemical analysis was found to contain 0.9 per cent by weight excess tellurium. Above 900 K the negative temperature coefficient of resistivity suggests the onset of intrinsic conduction with $\rho \propto e^{0.7/2kT}$, for kT expressed in ev.

Without exception, specimens of the 3-4 composition are n-type with free-electron concentrations in the range 10^{20} to $10^{22}/cm^3$ and $R_H\sigma$ values <1 cm^2/volt-sec. It is noted that, if the rare-earth elements are present as trivalent ions, it is possible that each molecular unit could contribute a free conduction electron. At 100 per cent ionization of the rare-earth elements, about 4 to 8×10^{21} electrons/cm^3 would be available for conduction.

As is shown in Figure 12 and Table 13 (in which the properties of representative specimens are given), corresponding compositions containing neodymium or other rare-earth elements exhibit properties which are generally similar to those of the gadolinium compounds.

TABLE 13. ROOM-TEMPERATURE ELECTRICAL PROPERTIES OF SELENIDES AND TELLURIDES

Synthetic Composition	Resistivity, ρ, ohm-cm	Hall Coefficient, R_H, cm^3/coulomb	Hall Mobility, μ, cm^2/volt-sec	Carrier Concentration, n, cm^{-3}	Seebeck[a] Coefficient, α, μ v/ K
Ce_2Se_3	3.4×10^{-3}	0.01	3.7	5.3×10^{20}	-57
Ce_2Te_3	145	-315	--	--	--
Gd_3Se_4	1.1×10^{-3}	Negative	--	--	-14
Gd_2Se_3	1.3×10^{-3}	Negative	--	--	-7
Nd_3Te_4	3.5×10^{-4}	Negative	--	--	-20
Gd_3Te_4	4.6×10^{-4}	Negative	--	--	--
Er_3Te_4	2.8×10^{-4}	Negative	--	--	--
Nd_2Te_3	0.31	+1.15	5	4.2×10^{18}	+180
Nd_2Te_3	1.2×10^{-3}	-0.008	6	8×10^{20}	-30
Nd_2Te_3	22	Negative	--	--	-260
Gd_2Te_3	1.9×10^{-2}	+0.34	18	1.9×10^{19}	+190
Gd_2Te_3	1.5×10^{-2}	+0.16	11	4×10^{19}	+160
Gd_2Te_3	2.0×10^{-3}	-0.11	55	5.7×10^{19}	-80
Gd_2Te_3	8.1×10^{-3}	-0.3	40	2×10^{19}	-60
$GdTe_2$ (melt-grown)	5.5×10^{-2}	Positive	--	--	--
$GdTe_2$ (vapor-grown)	1.79	+2	1.3	2.7×10^{18}	--
$CeSe_2$	292.0	Positive	0.4	5×10^{16}	+[illegible]

(a) Seebeck coefficient values were determined at temperatures 20 to 40°C above room temperature.

It is worthy of note that the M_2X_3 compositions exhibit rather typical semiconducting properties, being obtainable as both n- and p-type materials and possessing higher resistivities and higher carrier mobilities, and, in the case of Gd_2Te_3 at least, showing the apparent onset of intrinsic conduction at higher temperatures. On the other hand, for the M_3X_4 compositions, no indication of a thermally activated conduction process has been obtained from resistivity data taken as a function of temperature in the range 77 to 1300 K; reliable Hall data could not be obtained at the generally high carrier concentrations. Both the resistivity and Seebeck coefficient for these materials showed a temperature dependence that appears similar to that of a metal.

The compounds which crystallize in the Th_3P_4 structure make up a family of materials, members of which are of interest as thermoelectric materials for power generators operated at high temperatures. The Th_3P_4 structure is body-centered cubic with 28 atoms per unit cell. The M_2X_3 compositions are considered to have a defect Th_3P_4 structure with 16 anions per unit cell and 10-2/3 rare-earth atoms per unit cell distributed at random over 12 equivalent sites. As additional rare-earth atoms are added, these vacant sites are progressively filled until the M_3X_4 composition is attained, corresponding to all sites filled.

At the 2-3 composition, formal charge balance prevails if the rare-earth element assumes a tripositive state. At the 3-4 composition, as many as four excess valence electrons are available per unit cell, or approximately 6×10^{21} electrons/cm^3.

One may adjust the carrier concentration, with a corresponding change in the vacancy concentration, by changing the composition of the compound in the range M_3X_4 to M_2X_3. Hence, the values of electrical resistivity and Seebeck coefficient may be adjusted to optimize the thermoelectric figure of merit $Z = \alpha^2/\kappa$, where α is the Seebeck coefficient and κ is the thermal conductivity. The carrier concentration also may be adjusted, without a change in the vacancy concentration, by replacing rare-earth elements with divalent alkaline-earth elements, such as barium or strontium.

The range of compositions of interest is shown in Figure 15, using the Ce-Sr-Se system as an illustration. In analyzing series of specimens at points along the two bold-face lines starting with the 3-4 composition and progressively replacing cerium atoms with vacancies or strontium atoms, electrical resistivity and Seebeck coefficient of the specimens increase in a regular manner. This suggests that carrier concentration decreases as the rare-earth atoms are replaced or as the concentration of excess valence electrons is decreased. In the limited number of cases in which Hall effect could be measured, carrier concentrations given by $1/R_H e$ were in fair agreement with the calculated number of excess valence electrons. The most interesting compositions for thermoelectric applications have been found in the regions of intersection of the cross-hatched region with the two bold-face lines. Actually, interesting compositions would be expected also within the cross-hatched region in which the normally vacant sites of the 2-3 composition are filled only partially with rare-earth and alkaline-earth atoms.

Table 14 shows thermoelectric data at 298 and 1300 K for representative compositions. The high-temperature thermal conductivities were estimated by considering (1) measured electrical resistivities, (2) the Wiedemann-Franz relationship, (3) the measured room-temperature thermal conductivities, and (4) high-temperature lattice thermal conductivities deduced from observed trends in this parameter for CeS-Ce_2S_3

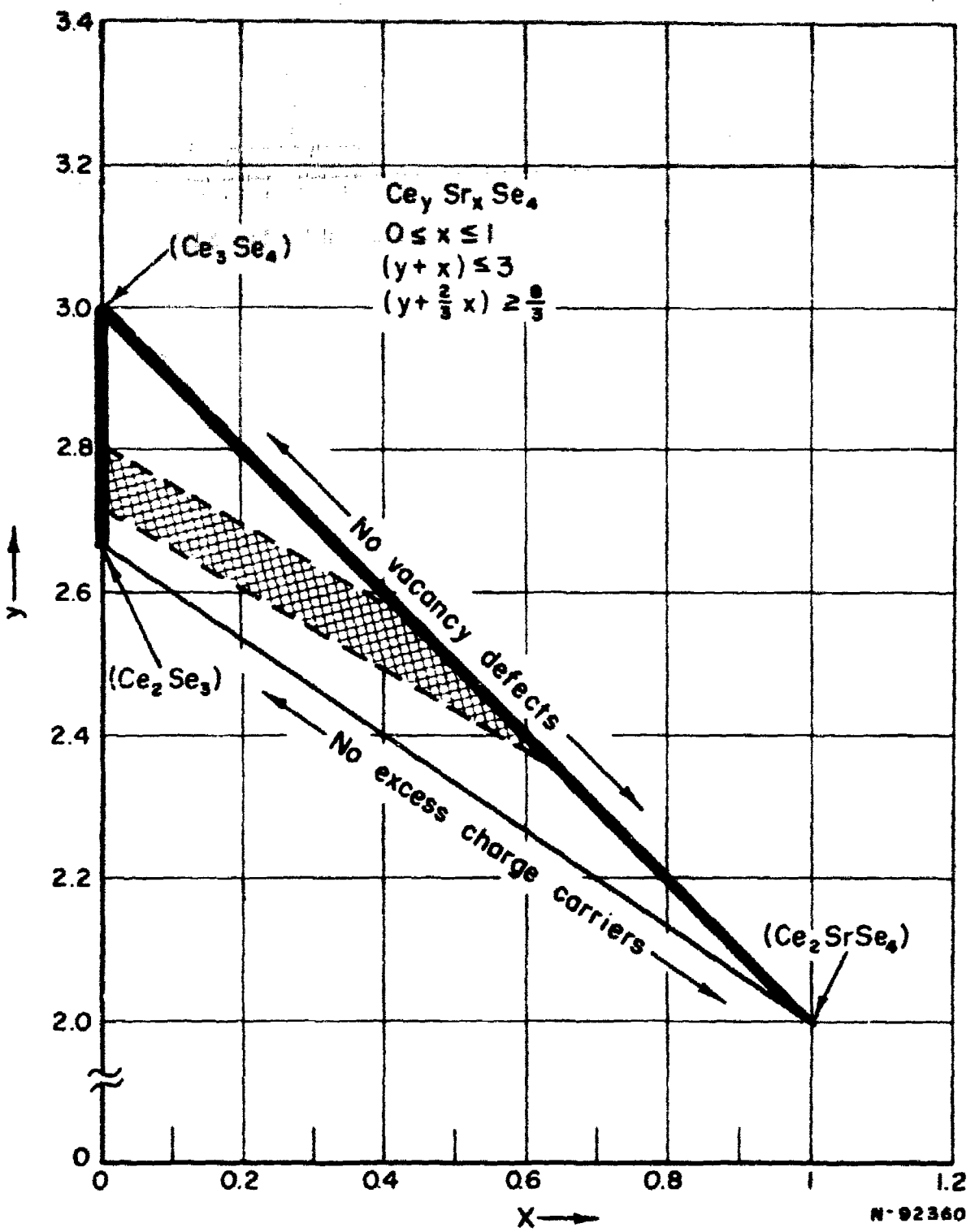

FIGURE 15. BOUNDARY CONDITIONS OF INTEREST FOR RARE-EARTH COMPOUND AND ALLOY COMPOSITIONS

compositions (Ref. 13). Estimates obtained in this manner are believed to be conservative. In view of the fact that no serious attempt has yet been made to optimize the material compositions, it is encouraging that ZT values greater than unity at 1000 C have been attained. High-temperature figures of merit of this magnitude are rare. Other similar work reported (Refs. 13, 14) has been limited to sulfides of rare earths with strontium or barium doping, and estimated ZT values of unity have been obtained with certain compositions. It has been observed that prevention of surface oxidation and application of contacts are more serious problems with the rare-earth sulfides than with the tellurides or selenides.

TABLE 14. THERMOELECTRIC DATA FOR REPRESENTATIVE RARE-EARTH COMPOUNDS AND ALLOYS

Synthetic Composition	T, K	ρ, ohm-cm	α, μV/deg	κ (a), watt cm-deg	ZT (Est.)
$Ce_{2.72}Se_4$	298	8.0×10		0.024	
$Ce_{2.4}Sr_{0.6}Se_4$	298	1×10^{-3}	-48	[illegible]	
	1300	4.0×10^{-3}	-200	0.015	0.9
$Ce_{2.5}Ba_{0.5}Se_4$	298	8.0×10^{-4}	-35	0.024	
	1300	1.7×10^{-3}	-140	0.026	0.6
$Ce_{2.5}Sb_{0.5}Te_4$	298	1.1×10^{-3}	-40	[illegible]	
	1300	4.0×10^{-3}	-210	0.018	1.0
$Nd_{2.76}Te_4$	298	1.4×10^{-3}	-40	[illegible]	
	1300	7.5×10^{-3}	-240	[illegible]	1.1

(a) Thermal conductivity, κ, at 1300 K was calculated as $\kappa = \kappa_{elec} + \kappa_{ph}$, where $\kappa_{elec} = LT/\rho$, $L = \frac{\pi^2}{3}\left(\frac{k}{e}\right)^2$, κ_{ph} (at 1300 K) $= \frac{1}{2}\kappa_{ph}$ (at 298 K), and $ZT = \alpha^2 T/\kappa\rho$.

Polyselenides and Polytellurides

Although compounds of the type MX_2 and MX_4 tend to dissociate at moderate temperatures, specimens of $GdTe_2$, $GdTe_4$, and $CeSe_2$ have been prepared by crystallization of melts under atmospheres of the metalloid vapor. The $GdTe_4$, so prepared, was in the form of leaflets embedded in a matrix of lower tellurides, and only crystal-structure studies on this material were undertaken. However, polycrystalline specimens of $GdTe_2$ and $CeSe_2$, large enough to permit electrical-property measurements, were synthesized. In addition, sizable single crystals of $GdTe_2$ were prepared by a vapor-growth method in which halogens were utilized to promote transport through the vapor phase.

The observed electrical properties (lower portion of Table 13) indicate that these compounds always exhibit p-type conduction, with resistivities being higher and the Seebeck coefficient generally lower than those of the p-type specimens of the M_2X_3 compounds. The results for $CeSe_2$ show a combination of high resistivity, negative TCR, low carrier concentration, and low carrier mobility, suggesting similarity to the samarium and ytterbium monoselenides in which ionic valences are balanced. In contrast, resistivity of the ditelluride of the normally trivalent gadolinium is low, while

Arsenides and Antimonides (Nd, Sm, and Gd)

The rare-earth elements form binary compounds with the elements of chemical Group V, arsenic and antimony, which contain nominally equiatomic portions of the elements and which crystallize in the fcc NaCl structure. Battelle's research on the arsenic and antimony compounds was confined to study of such compostions, and no investigation was made of the possible existence of other compounds or phases in these binary systems. Electrical properties of representative specimens of the compounds are shown in Table 15. All specimens measured have been n-type. If carrier concentrations are calculated using the simple $1/R_H e$ relation, where R_H is the Hall coefficient and e the charge on an electron, large free-electron concentrations in the range 4×10^{20} to $2 \times 10^{21}/cm^3$ are obtained. Nevertheless, the electron mobilities determined from $R_H \sigma$, where σ is the electrical conductivity, are seen to be large relative to other rare-earth compounds studied in this research.

TABLE 15 OBSERVED ELECTRICAL PROPERTIES OF NdAs, GdAs, SmAs, AND NdSb

Sample	Synthetic Composition	Temperature T, K	Resistivity, ρ, 10^{-3} ohm-cm	Mobility, μ, $cm^2/v\text{-}sec$	Carrier Concentration, n, 10^{20} cm^{-3}	Seebeck Coefficient, α, $\mu v/deg$
12R	NdAs	310	0.21	76	4.0	-22
		97	0.12	130	4.2	-8
32RA	NdAs	309	0.155	87	4.7	-9
		102	0.054	270	4.3	-2
29R	NdAs	304	0.142	86	5.2	-11
		106	0.087	140	5.2	-4
36R	NdAs	309	0.15	30	12	-3
39R	GdAs	305	0.12	70	8.0	-13
		110	0.076	90	8.6	-6
44R	SmAs	306	0.19	50	6	-5
		104	0.13	70	7	-2
47R	NdSb	300	0.076	40	20	
		130	0.045	70	20	

The electrical properties of SmAs prepared using purified samarium were found to be substantially the same as for SmAs prepared with as-received samarium metal. Thus, it appears that impurities initially present in the commercial rare-earth metals are not contributing a significant portion of the free carriers. One can make the same

[illegible] rations. However, these compounds are prepared under extremely severe conditions (e.g., at temperatures near 2500 C), and it is distinctly possible that electrically active impurities are introduced from components of the system in the course of the high-temperature preparation.

Spectrographic analysis of a SmAs specimen revealed the presence of significant levels of silicon, tantalum, and copper: concentrations of 2000, 2000, and 400 ppm (atomic), respectively (compared with approximately 130, 400, and 60 ppm, respectively, in the starting materials). If the silicon and tantalum act as donor impurities, the concentration of each element could account for about 1×10^{20} electrons/cm^3, which is still somewhat smaller than the measured carrier concentration of this particular sample ($n = 8 \times 10^{20}/cm^3$). The source of tantalum is no doubt the tantal[illegible] tube which holds the SmAs charge. The source of silicon and copper may be the quartz envelope used in the preparation. The carbon and oxygen concentrations in this sample have not been determined. However, it appears that one must look at other possibilities in addition to chemical impurities for the origin of the high free-electron concentrations.

The results of chemical analysis of several NdAs specimens indicate that the specimens tend to be arsenic deficient. For example, analysis of Specimen 42RA, which was prepared with excess arsenic and subsequently sintered in arsenic vapor at 1 atm of pressure, gave a composition of $NdAs_{0.994}$. Specimen 46R apparently lost arsenic in preparation, going from a synthetic composition of $NdAs_{0.97}$ to a final composition of $NdAs_{0.96}$. Carrier concentrations obtained from the electrical measurements on the two specimens (see Table 15) reflect the differences between compositions of the samples, suggesting lattice defects as one possible source of the high carrier concentrations.

Figure 16 shows the temperature dependence of $R_H\sigma$ for these materials. The large concentrations of charged carriers present suggest the possibility of large concentrations of ionized scattering centers which would suppress the mobility of electrons in these materials. However, using the simple relation $R_H\sigma$ for mobility, one sees that this is not the case. Relatively high mobilities are obtained, being on the order of 100 cm^2/volt-sec for the arsenides at room temperature, with a temperature dependence suggesting that a lattice scattering mechanism dominates. This latter is in agreement with the above-discussed conclusion from analytical data to the effect that lattice defects rather than ionized-impurity centers are the primary sources of change carriers.

THIN FILMS

The preparation and study of rare-earth metals and compounds in film form were undertaken with full recognition of the magnitude of the task and of the fact that the base upon which the technology could be built (i.e., the technology of the bulk materials) was not well developed. It was recognized that purity and crystalline state of the materials, over which little measure of control has as yet been established, would have even more profound effect on properties of the films than on those of the bulk materials. In addition, at the inception of the research program, it also was recognized that only a beginning could be made within the time available in this contract period. It was

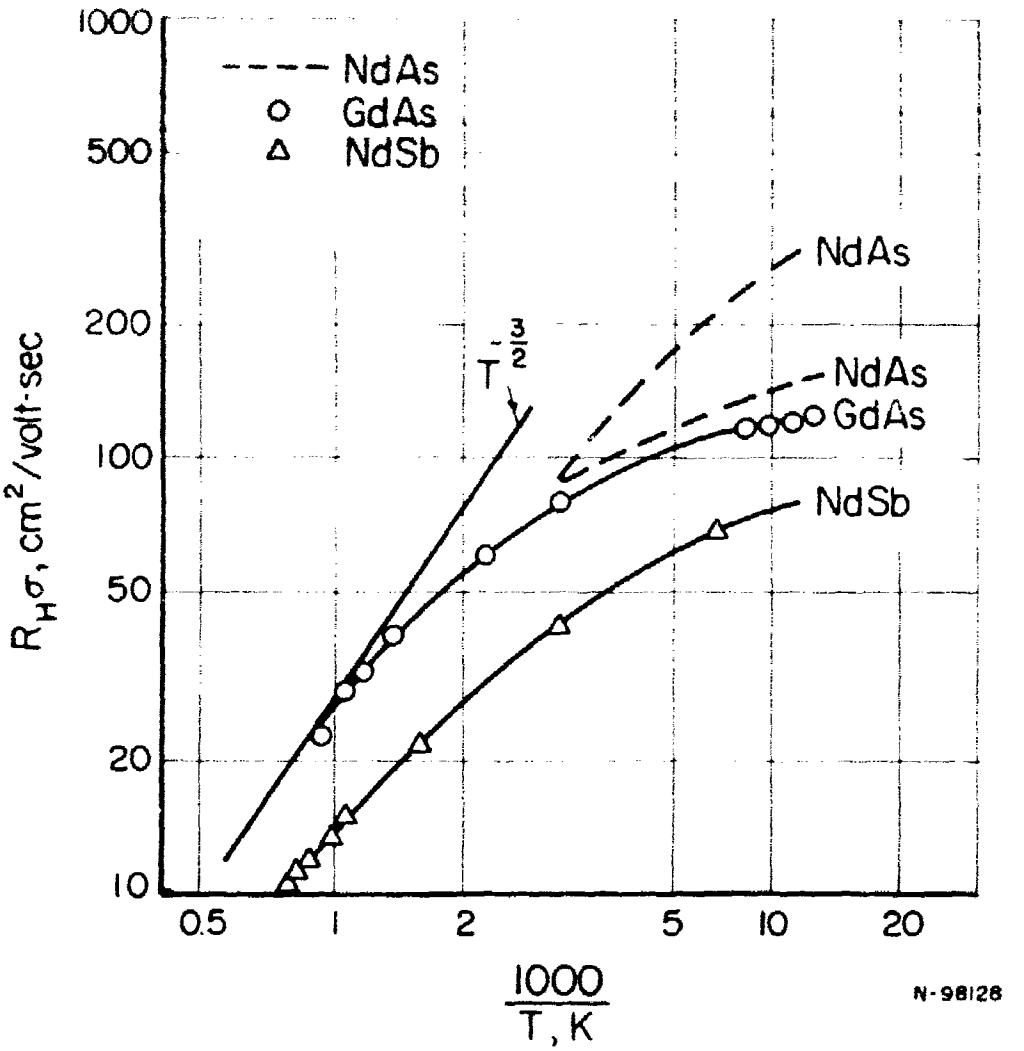

FIGURE 16. HALL MOBILITY AS A FUNCTION OF TEMPERATURE FOR N-TYPE NdAs, GdAs, AND NdSb

Preparation of Arsenides and Selenides

The preparation and study of films of the rare-earth arsenides and of rare-earth compounds containing selenium were undertaken with the ultimate objective of making these potentially useful electronic materials available in thin-film form. In the initial experimental work which is discussed here, thick films (2.5 to 170 μ) were prepared so that synthetic techniques could be evaluated by comparing properties of the films with those of the bulk materials.

The preparation method, which was utilized primarily, involved: (1) the formation of a film of the rare-earth metal by vacuum deposition, and (2) the reaction of the rare-earth-metal film with vapor of the metalloid at moderate temperatures (475 to 1000 C).

In connection with the film-preparation work, some study was made of the possibility of obtaining vapor transport of the compounds which could be utilized for the film deposition. The results of experiments with SmAs, utilizing small concentrations of I_2 to generate a volatile samarium compound, were negative. Although vapor transport of samarium iodide was observed at 850 C, no vapor transport of SmAs was observed in either direction along a temperature gradient (e.g., in 48 hours at 670 to 900 C). This is in agreement with results obtained in the studies on the vapor-growth of crystals (of selenides and tellurides) which are discussed in a preceding section and which indicated that rates of transport of the subject rare-earth compounds are extremely low in these types of chemical systems.

To carry out the film preparation as initially described, a vacuum system, such as is shown in Figure 17, was designed and constructed. The essentials were the two sidearms, the substrate holder attached to a magnetic susceptor, and the suspended tantalum crucible containing rare-earth metal, with provisions for induction heating of the latter. The substrate first was held in a sidearm and was baked out in the movable resistance furnace. The rare-earth-metal source was degassed and the system was gettered by distilling some rare-earth metal. Next, the substrate was moved into place for deposition of the metal film. The film then was moved into the second, evacuated sidearm, containing an excess of arsenic or selenium and was dropped from the holder. Finally, the sidearm containing the specimen was sealed off, removed, and placed in a furnace where the metalloid vapor was reacted with the rare-earth metal film.

Film thickness was controlled by controlling the time and (source) temperature for deposition of the rare-earth metal film. Thickness of the resulting film of the compound usually fell within ± 20 per cent of the desired value and was in the thickness range of interest. For example, in a series of six films, thickness ranged from 4 to 6 microns. The thicknesses of the films were determined with an optical microscope having a calibrated eyepiece. Cross sections required for the purpose, which were not appreciably distorted, were obtained by fracturing the substrate (and the film). Three types of substrates were utilized: (1) dense, high-purity, ceramic alumina, (2) cleaved,

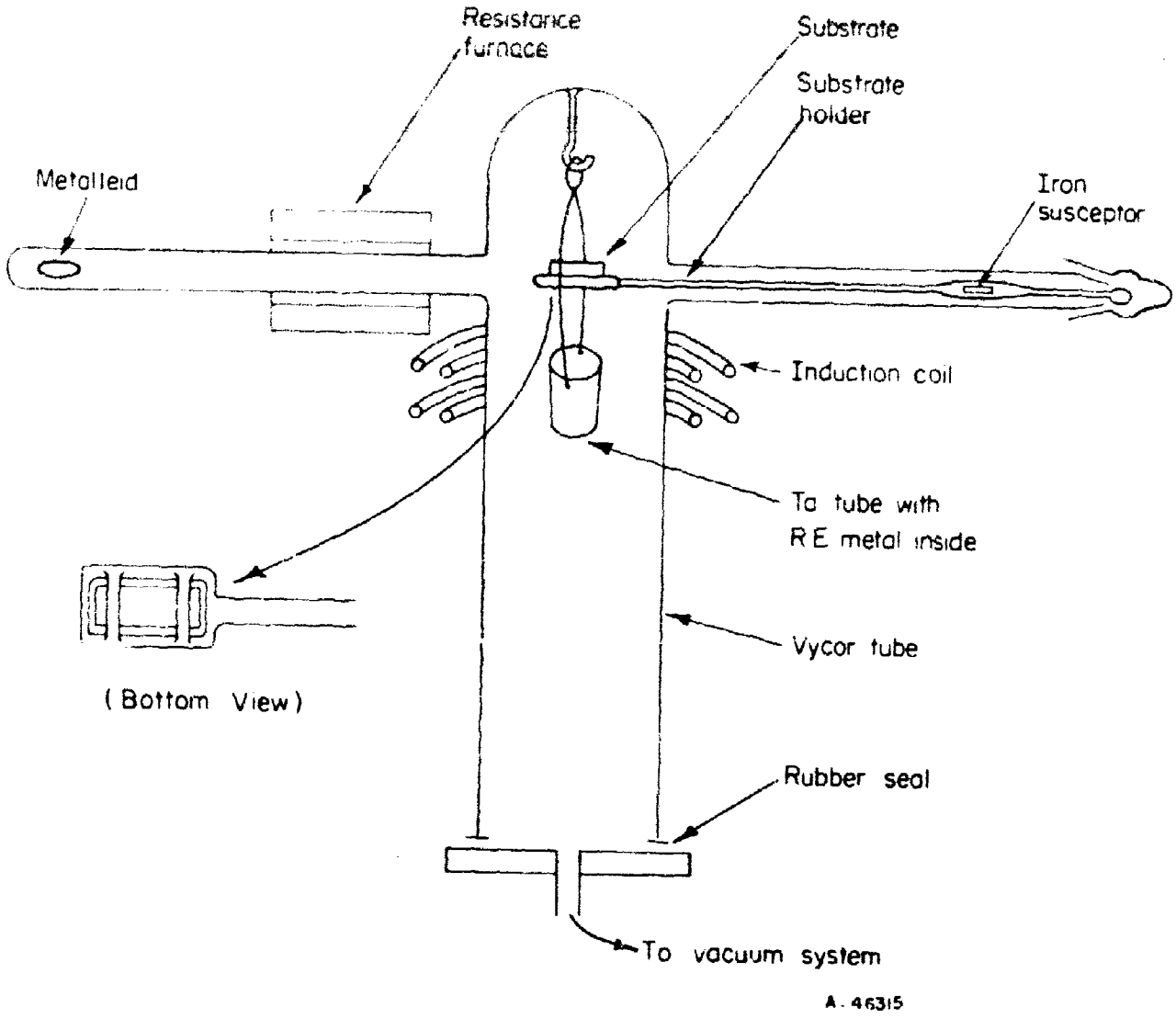

FIGURE 17. VAPOR-DEPOSITION APPARATUS

[illegible] Al_2O_3 and the crystalline MgO present [illegible] surfaces obviously will always contain some porous regions, while the [illegible] on the crystalline MgO constitute undesirable surface features.

Illustrative data on the film preparations, which are given in Table 16, show that it was possible to prepare films of the arsenides with properties very similar to those of the bulk solid. In the case of the selenide films, however, one encounters a stoichiometry problem: the films prepared at low temperatures (500 to 600 C) in the presence of selenium were found to be the polyselenide, MSe_2, while at the higher temperature (1000 C) the sesquiselenide phase was obtained. These results are in accord with the results of the phase-relationship studies and with observations made in the course of the preparation of the bulk materials.

Electrical resistivity versus temperature and optical transmission data were taken on the sesquiselenide phase; both sets of data indicated that the conductivity in the range around room temperature is dominated by an impurity-activation energy of ~0.35 ev.

The results for Reactions 74R and 111R show very clearly the reactivities of the rare-earth metals. In both cases, the metal films were taken to elevated temperatures when concentrations of the metalloid vapors were very low, and in both cases the metals reacted with the substrate materials producing material with unexpectedly high electrical resistance. That this involved reaction with the substrate was substantiated by examining a film of gadolinium metal on crystalline MgO which had been taken to 1080 C (as Film 74R), in vacuum; the film was found, by X-ray diffraction, to be polycrystalline and no longer gadolinium metal but another unidentified phase.

The reaction times used are believed to be far in excess of the minimum time required to get essentially complete reaction. No attempt was made to determine the minimum time or to shorten the procedure. It was felt that the use of excessively long high-temperature treatments would have a salutory effect on specimen homogeneity.

Preparation of Oxides

From a review of previous work on the preparation of metal oxides (especially rare-earth oxides), it appeared that it would be possible to prepare rare-earth oxide films by the direct reaction of oxygen with the metal. However, little or no information was available regarding the nature of rare-earth oxide films. Hence, an experimental investigation of these materials appeared to be advisable.

The first step taken in the preparation of thin oxide films was to prepare a smooth metal surface prior to the oxidation. The two methods used in preparing smooth surfaces were (1) to polish a piece of bulk metal using Al_2O_3 ($\leq$ 0.3-μ particles) in kerosene for the final polish and (2) to vapor-deposit a layer of metal (a few microns thick) onto a smooth substrate. Cleaved single crystals of MgO and the fused surfaces of Vycor

TABLE 16. SUMMARY ON THE PREPARATION OF FILMS OF RARE-EARTH COMPOUNDS

[illegible]	Substrate	Reaction Conditions: Substrate Temperature, C	Reaction Conditions: Pressure of Metalloid Vapor, atm	Reaction Conditions: Reaction Time, hr	Film Characteristics: Thickness, microns	Film Characteristics: Electrical Resistivity, ohm-cm	Remarks
[illegible]	Al_2O_3 ceramic	650	[illegible]	22	13	9×10^{-4}	
	Ditto	850	~0.5	15	11	4.9×10^{-4}	
	"	1000	0.5	6	15	4.9×10^{-4}	
	"	1150	~1.5	19	2.5	4.6×10^{-3}	
	Cleaved MgO crystal	1080	0.13	48	10	5×10^{-4}	
	Ditto	1080*	0.13	26	6.5	2.2	Polycrystalline, but high degree of orientation on substrate (by X-ray diffraction)
[illegible]	--	--	--	--	--	1.2×10^{-4}	
[illegible]	Cleaved MgO crystal	970	1.5	66	170	1.7×10^{-4}	
[illegible]	--	--	--	--	--	1.5×10^{-4}	
[illegible]	Al_2O_3 ceramic	500	0.001	45	0.6	129	
	Cleaved MgO crystal	500	0.001	51	5	710	
	Ditto	500	0.0001	45	12.5	210	
	"	500	0.003	~60	5.5	408	$SmSe_2$ by X-ray diffraction
	"	500	"	~51			
	"	500	10^{-5} atm	~45		7×10^8	Sm_2Se_3 by X-ray diffraction. $\sigma_{light}/\sigma_{dark} = 3.76$
	"	500	10^{-5} atm	~39			
	"	1000	10^{-5} atm	~44			
	--	--	--	--	--	1400	

*Substrate heated before selenium-vapor atmosphere was generated.

[illegible] the MgO [illegible] C [illegible] were baked at 220 C in the resistance furnace encompassing [illegible] of the apparatus. To clean the metal surface, the metal, which was contained in a tantalum tube, was evaporated partially before exposing the substrate. The substrate was then pulled into position over the tantalum tube by pulling the substrate holder with a magnet. The rare-earth metal was then vapor-deposited onto the substrate.

Oxidation was accomplished by heating the polished bulk metal or vaper-deposited metal in an oxygen stream in a resistance furnace designed for the experiments. In exploratory experiments to determine suitable conditions for film preparation, the temperature of the metal was increased at a rate of 2 C/min, and interference colors associated with the rare-earth oxide were observed through a slit in the resistance furnace. After the furnace had reached the desired peak oxidation temperature, it was allowed to cool rapidly. Figure 18 shows the interference colors observed at the various temperatures during the oxidation (at 1 atm of oxygen pressure) of gadolinium, erbium, samarium, and yttrium metals. The apparent order for increasing resistance to oxidation among the types of metal specimens employed is: polished gadolinium, polished erbium and samarium, vapor-deposited yttrium, vapor-deposited gadolinium, and polished yttrium. Microscopic observation of the surface of the oxide films indicated that areas of the surfaces of a given specimen were oxidizing at different rates, since several interference colors were seen with each specimen.

Precise correlation between the interference color and film thickness cannot be made without reasonably comprehensive information on (1) the refractive index of the film, (2) the effect of the metal-oxide interface on the reflected light, and (3) the widths of the intereference bands. However, the order of magnitude of the thickness can be estimated from data on other kinds of films (Ref. 15). Estimates made of the thicknesses of the rare-earth oxide films prepared in this work are in the range, 100 to 3000 A.

Oxide films were also produced on yttrium by anodizing the metal in a 4 per cent boric acid solution using 1-1/2 to 4-1/2 volts. In order to get the reaction to proceed over the entire metal surface, it was found necessary to clean the surface by swabbing it with NaOH solution until it would be wetted uniformly with water. As in the case of oxides formed by solid-vapor reaction, the oxides formed by anodization contained areas which were oxidized at different rates.

To put the evaluation on a firmer basis, the nature of yttrium metal surfaces prepared under various conditions was investigated. It was found that the grain size was brought out nicely by etching for a short time using 1 per cent nitric acid in ethanol or by heating in oxygen, or to a lesser degree by anodizing in boric acid. The following conclusions were drawn from observations of photomicrographs taken under magnification of 600X. The vapor-deposited yttrium metal was blemish free (see Figure 19a), whereas the bulk metal, which was polished with Al_2O_3 in kerosene, showed a high density of blemishes (see Figure 19b), which could be removed by etching. Figure 20 shows the comparison in grain sizes obtained for various preoxidation treatments. The grain sizes of the polished bulk metal (see Figure 20a) and the metal vapor deposited onto a single crystal of MgO (see Figure 20b) were about the same. However, the grain

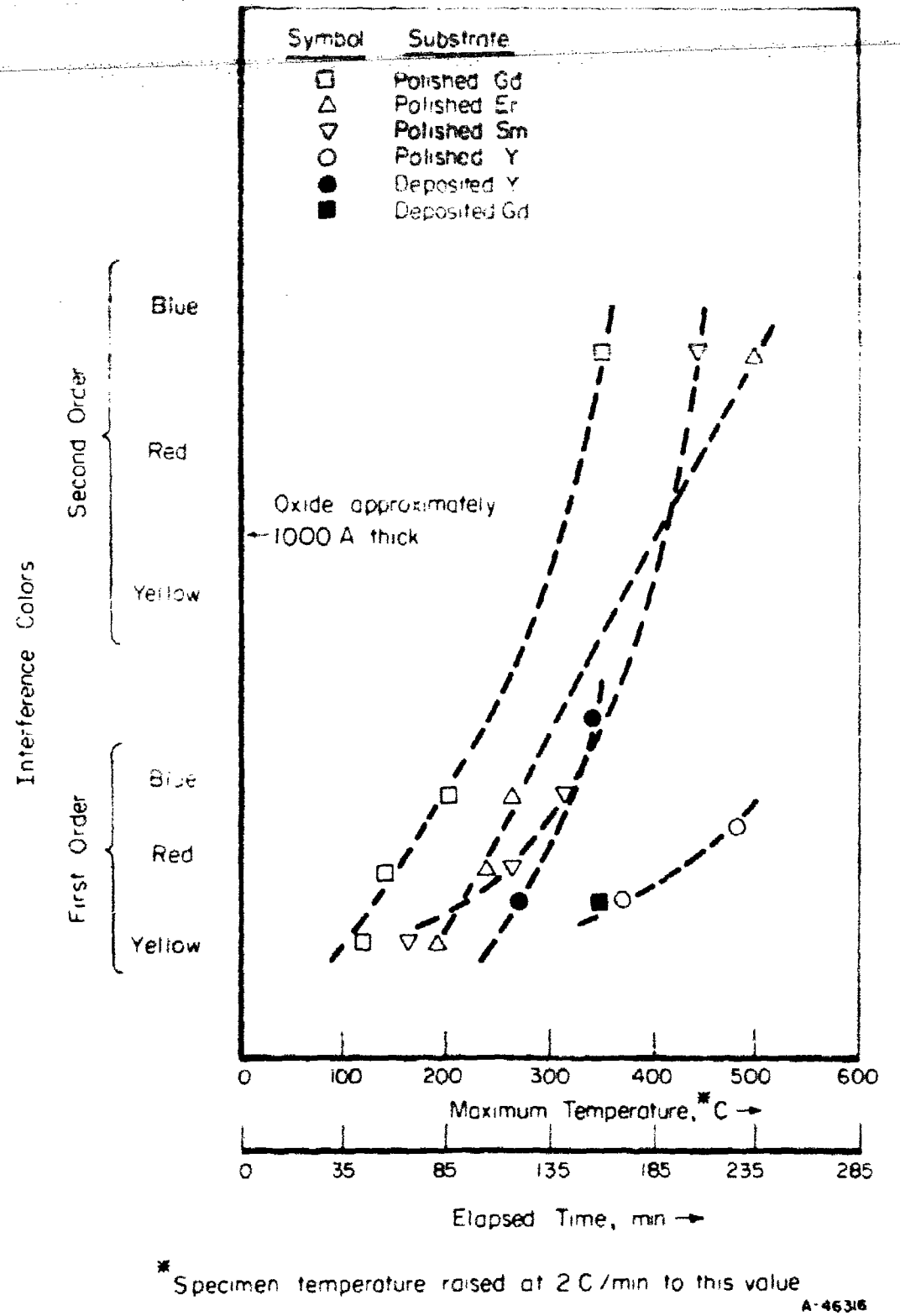

FIGURE 18. INTERFERENCE COLORS OBSERVED IN THE PREPARATION OF OXIDE FILMS

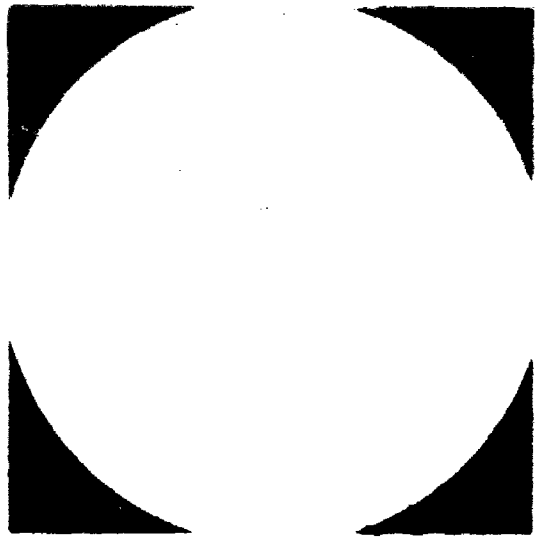

a. Vapor Deposited on Glass

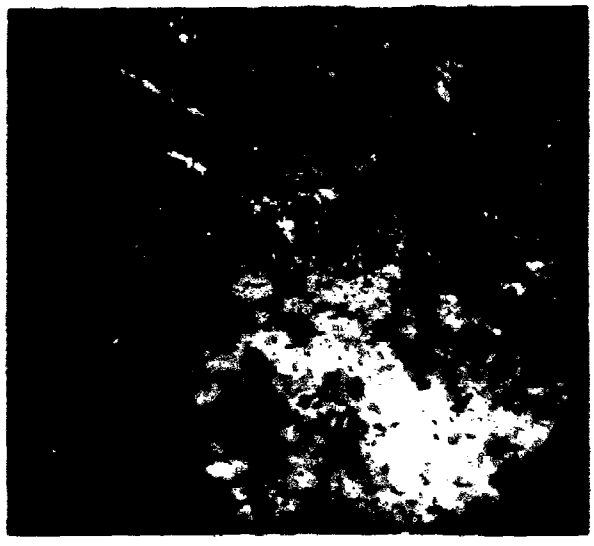

b. Polished

FIGURE 19. AS-PREPARED SURFACES OF YTTRIUM METAL (600 X)

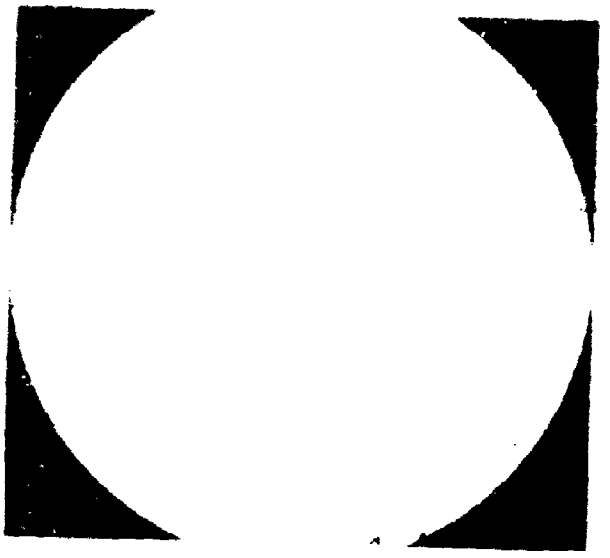

a. Polished

b. Vapor Deposited on MgO

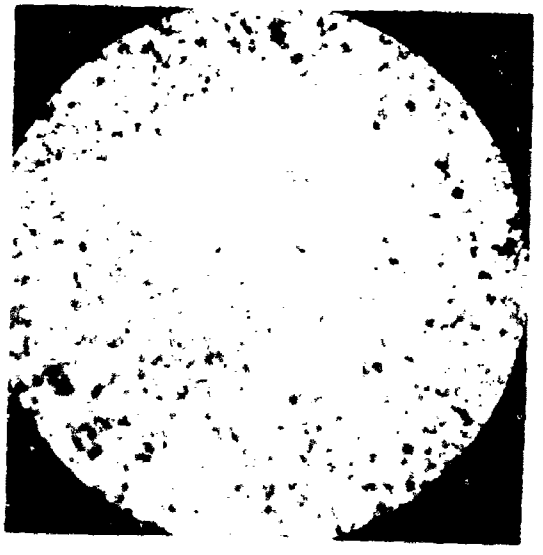

c. Vapor Deposited on Glass

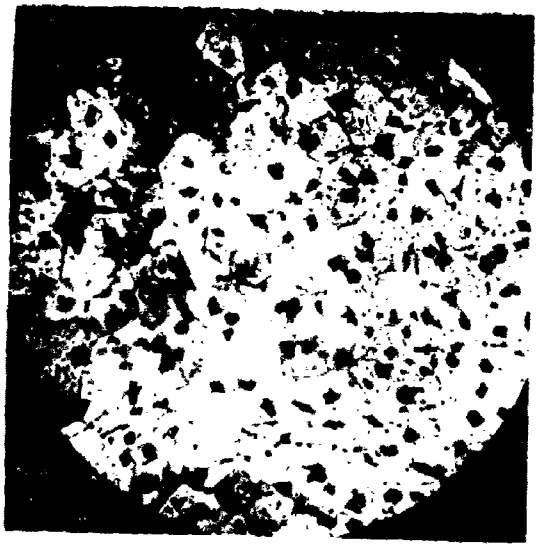

d. Polished and Annealed

FIGURE 20. ETCHED SURFACES OF YTTRIUM METAL (600 X)

size of the metal vapor deposited onto glass (see Figure 20c) was several times larger in average diameter, and the grain size of the bulk metal after the sample was annealed at 900 C for 1 hour and cooled slowly was many times larger, ca 50 times (see Figure 20d). No experiments were conducted on the annealing of the vapor-deposited metal. The surface of the annealed bulk metal showed some dark areas which were subgrain size. These dark areas appear to be a precipitated phase in the metal, since they remain when the surface is ground away and the metal is repolished.

Although all rare-earth oxide films prepared to date have been nonuniform in thickness, as discussed previously, some qualitative comparisons can be made among the various materials and preparative techniques used. Essentially no differences are noted which would suggest that oxidizing one rare-earth metal yields a more uniform film than oxidizing another. Likewise, oxide film uniformity does not appear to depend on maximum temperature for the solid-vapor reaction, on the temperature-time program employed for the reaction, or whether or not the metal is exposed to the atmosphere prior to oxidation. On the other hand, less uniform films consistently are produced when polished metal surfaces are oxidized, compared with vapor-deposited metal surfaces. The sizes of the crystal grains apparent on these surfaces are about the same. However, one might expect the grains present in the vapor-deposited metal to have a tendency to be oriented during growth so as to have fewer different crystallographic faces exposed during oxidation. In addition, one would expect the polished surface to be in a highly strained condition because of work damage, and it may be less smooth than the vapor-deposited metal surface. One or both of these factors might influence the oxidation and produce the observed difference. To this point, it is noted that a more uniform oxide film is produced on a polished surface after the metal has been annealed at 900 C for 1 hour. Of course, in addition to removing the effects of work damage, the anneal produces grain growth which may lead to more uniform oxide films if the grains surviving tend to be oriented similarly. The solid-vapor reaction and the anodization have produced oxide films of comparable uniformity.

Contacts to the oxide films were made (1) with air-dry silver paint, (2) with vapor-deposited gold and (3) with vapor-deposited rare-earth metal. The lateral dimensions of the samples were large enough that, in some cases, a series of contacts could be applied to the oxide, thus giving a number of metal-oxide-metal units on each sample.

One of the experimental difficulties encountered in this initial work was that of poor bonding between the oxide film and the metal contacts which were vapor deposited onto the oxide film. It was found that this difficulty was alleviated when the preparation of oxide and vapor-deposition of yttrium contacts onto the oxide were both carried out in the same apparatus with no interim exposure to the atmosphere. The difference observed may have been due to the influence of moisture on the surface of the oxide exposed to the atmosphere.

To obtain basic information as an aid in the evaluation of the Y_2O_3 films, dense bulk material was prepared. A bulk specimen of Y_2O_3 was prepared by heating powdered oxide at 800 C to remove water, pressing hydrostatically at 100,000 psi, and sintering at about 2400 C for 10 minutes in a tantalum tube. The density of the sintered oxide specimen was determined to be 4.63 ± 0.01 g/cm^3, 92.5 per cent of the theoretical density from X-ray diffraction data. The resistivity and low-frequency dielectric constant of this Y_2O_3 specimen have been measured. The resistivity was obtained over

the temperature range 100 to 160 C. In this range ρ varied as $e^{1.22/kT}$, the value at 100 C being 1.05×10^{10} ohm-cm. Extrapolation back to room temperature gives a value for this parameter of about 10^{14} ohm-cm.

The static dielectric constant was measured and found to be 11 between 100 and 100,000 cps, the loss tangent decreased from 0.00975 to 0.0005 over the same frequency range. Chang (Ref. 16) reports a refractive index of 1.93 for single-crystal Y_2O_3. This would give an optical dielectric constant of about 3.7 for the material.

Properties of Metal-Insulator-Metal Structures

Current flow between metal electrodes separated by a thin insulating region can be established via the following processes (Ref. 17):

(1) Direct tunneling of electrons from one metal to the other

(2) Thermionic emission over the metal-oxide contact barrier into the conduction band of the insulator

(3) Tunneling through the contact barrier into the conduction band of the insulator

(4) Tunneling of electrons directly from the metal to impurity or defect levels in the insulator and subsequent excitation of these electrons into the conduction band.

Process (1) has been investigated theoretically by numerious investigators, most recently by Simmons (Ref. 18) who calculated the current density versus voltage, J-V, characteristics over the entire voltage range and included the effects of dissimilar electrodes. Meyerhofer and Ochs (Ref. 17) adequately described current flow through thin films of Al_2O_3 and BeO in terms of Process (1) by adjusting barrier parameters to produce a calculated J-V curve which agreed quite well with their experimental data over much of the voltage range.

Similarly, the theory for Process (2) has been worked out, and use of this (Schottky) emission phenomenon is made in varactor diodes, for instance.

Process (3) is, in reality, a limiting case of Process (1) and occurs at biases such that the applied voltage is greater than the barrier height at the metal-insulator boundary.

Process (4) does not appear to have been treated in any great detail in the literature, but it is suggested in Reference (17) that the over-all effect would be a reduction in metal-metal tunneling brought about by an effective increase in the barrier height due to space charge buildup.

Thus, the analytical tools are available and under conditions such that one mechanism is dominant, quantitative information regarding effective barrier heights and thicknesses can be obtained from analyses of the J-V data. In practice, however,

certain experimental difficulties are sometimes encountered. Among these are the presence of shorting paths through the insulating film, and instability of the J-V characteristics due to surface phenomena or poor physical and electrical contact at the metal-insulator boundary. Similarly, the analysis is complicated by the addition of such unknowns as nonuniformity of the films, the presence of impurities or traps, and the use of dissimilar-metal electrodes.

The structures studied in this investigation were prepared by the methods discussed previously. The rare-earth metal (bulk or vapor-deposited base) served as one electrode, the other being either vacuum-deposited gold or rare-earth metal* or air-dry silver paint. As was already mentioned, when the base-metal electrode was a film, it was several microns thick. The oxide films were 100 to 3000 A thick. Effort was especially devoted to the development of procedures for the preparation of structures with both electrodes of the same rare-earth (yttrium) metal, since analysis of J-V characteristics is least complicated for such structures. Lead wires were attached using either silver paint or a low melting In-Ga alloy. Current voltage characteristics were obtained by a point-by-point technique or from a Tektronix transistor curve tracer.

The presence of shorting paths was indicated in most of the structures prepared during this investigation. In some cases, these could be "burned off" by passing relatively large currents through the structures for short periods of time. The contact problems, however, were not so easily solved. In addition to the instability and nonreproducibility of the characteristics, there was always doubt as to the true (electrical) contact area and hence uncertainty in the current density. For this reason, Battelle's results are presented in terms of I-V rather than J-V characteristics.

Typical examples of such characteristics are shown in Figure 21 and 22. Figure 21 shows the I-V characteristics for Gd-Gd_2O_3-Ag structures 124 RA and 124 RB, formed on polished gadolinium metal oxidized to 355 and 190 C, respectively. Although the I-V curves for these specimens both have the same shape, the curve for 124 RA lies above that for 124 RB. Assuming the thickness of the oxide layer to be the controlling factor, the reverse should be true since the oxide layer was formed at a higher temperature on Specimen 124 RA.

This discrepancy may arise in part from a difference in true contact area between the two structures, or be a manifestation of nonuniform film thickness. It may be observed, however, that the general features of metal-metal tunneling are indicated by these curves, i.e., ohmic behavior at low voltages and rapidly increasing current at higher voltages. That significant departures from ohmic behavior are observed only at voltages greater than 1 volt indicates a high barrier, possibly 3 ev, while the magnitude of the current indicates that the barrier is also narrow [see Figure 7 of Reference (18) for instance].

Most data on Y-Y_2O_3-Ag structure 128 RA, the basic structure of which was prepared by the oxidation of a vapor-deposited yttrium film to 370 C, gave curves similar to those for 124 RA and 124 RB. On the other hand, Figure 22 shows the I-V characteristics observed in one case for the structure 128 RA, which predict a very low barrier. The experimental points can be fitted over the initial portion of the curve by an equation of the form $I = K_1\left(\frac{V}{K_2}\right)^2 e^{-K_2/V}$. This is the same functional relationship occurring in

*Yttrium is often considered to be of the rare-earth group.

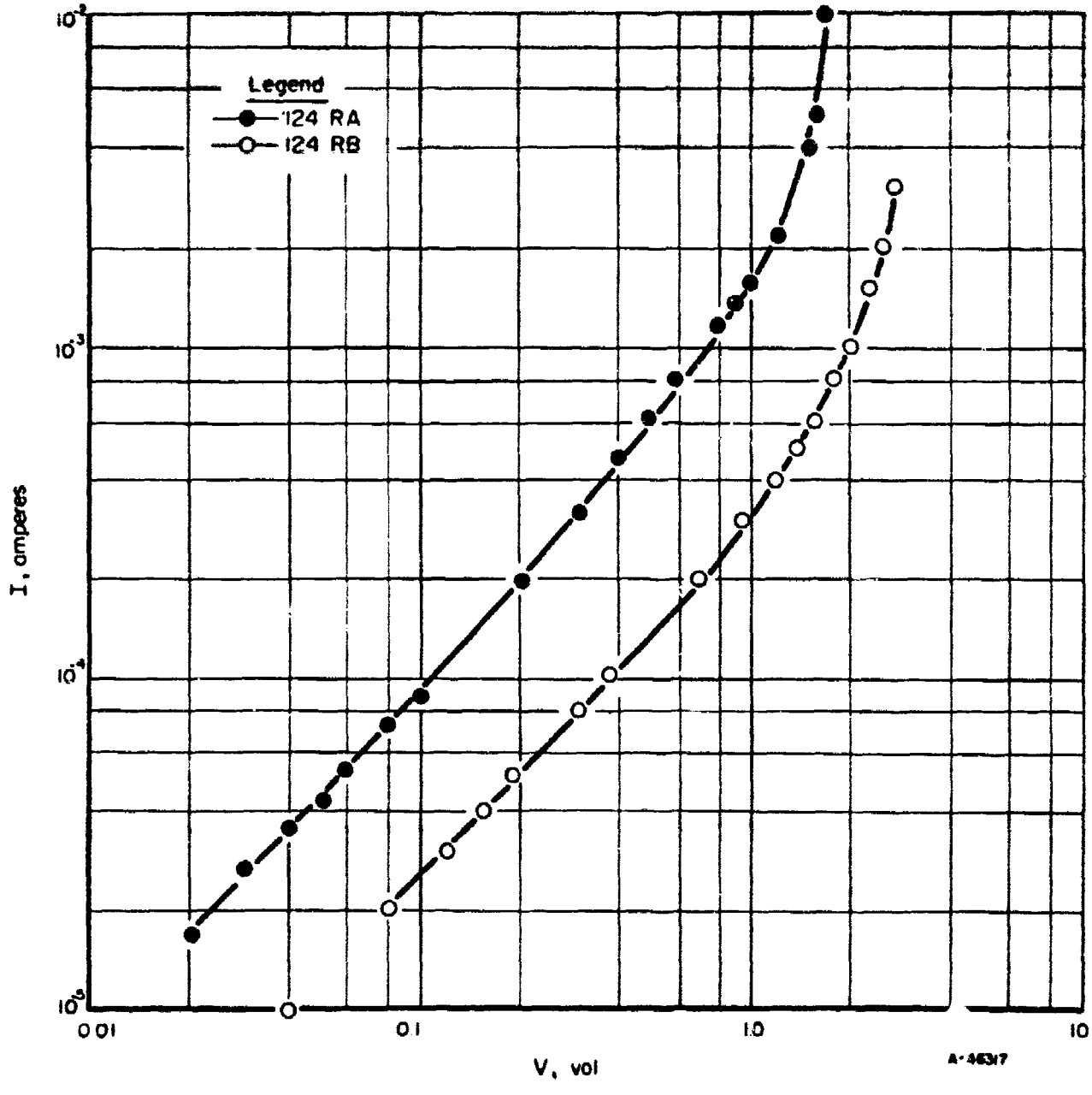

FIGURE 21. I-V CHARACTERISTICS OF Gd-Gd_2O_3-Ag STRUCTURES AT ROOM TEMPERATURE

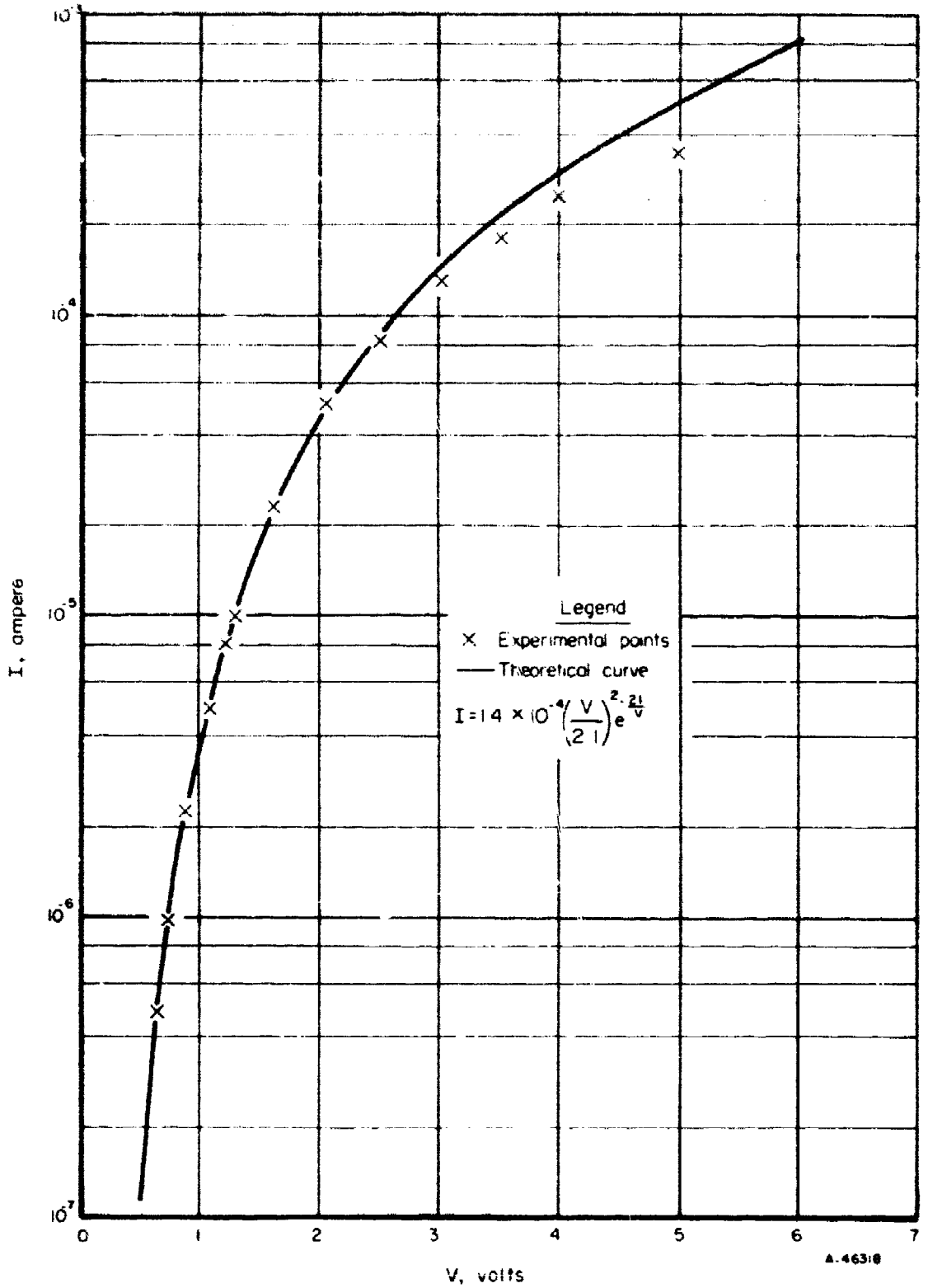

FIGURE 22. I-V CHARACTERISTICS OF Y-Y_2O_3-Ag STRUCTURE AT ROOM TEMPERATURE

tunnel emission. This suggests that the effective barrier height at the Y-Y_2O_3 interface is smaller than the lowest voltage for which data were obtained (~ 0.6 ev). One possible explanation for this inconsistency is that the presence of interface states is dominating the characteristics of these structures. In many specimens, difficulty in maintaining physical contact between the oxide and the foreign metal electrodes was encountered. In still other specimens, the surface of the oxide layer appeared to be highly conducting. Surface contamination could account for these effects and such contamination is possible since all of the structures were exposed to the atmosphere during some stage of the processing.

Before a meaningful assessment can be made of the properties of these materials, there is a need for more extensive investigation of the mechanism of oxide growth and for more precise control over the experimental techniques employed during processing and measurement.

POTENTIAL DEVICE APPLICATIONS

Although electronic-grade rare-earth metals are not yet available, and, problems connected with control of stoichiometry remain, the eventual utilization of rare-earth compounds and alloys in electronic applications is definitely indicated. Studies to date have indicated diverse applications for rare-earth compounds and alloys including thermistor and related devices, power-generation devices, and active devices, including "tunnel-emission" devices as well as the more conventional p-n junction device. Of these, realization of p-n junction devices utilizing rare-earth compounds is most speculative at this time. However, the rare-earth compounds with Group V-A anions appear to be a class of refractory, moderately-high-mobility semiconductors of potential interest for active device components.

Thermistors

As has been shown, the rare-earth monoselenide and monotelluride compositions, in which the rare earth is one such as samarium and ytterbium (and probably europium) that readily exhibits a +2 oxidation state, have relatively large room-temperature resistivities and exhibit large negative temperature coefficients of resistance (TCR). The materials are of special interest because of their high melting points and good thermal stabilities which indicate the feasibility of high-temperature (500 to 800 C) operation of thermistor-type devices made with these materials.

Figure 23 is a plot of specific resistance as a function of temperature for SmSe, YbSe, and typical commercially available thermistors. It is seen that the TCR's of the experimental samples of SmSe and YbSe compare favorably with those of the commercial thermistors and, in addition, it is indicated that thermistors based on these still-to-be-optimized materials could be operated over a much broader temperature range, extending to considerably higher temperatures.

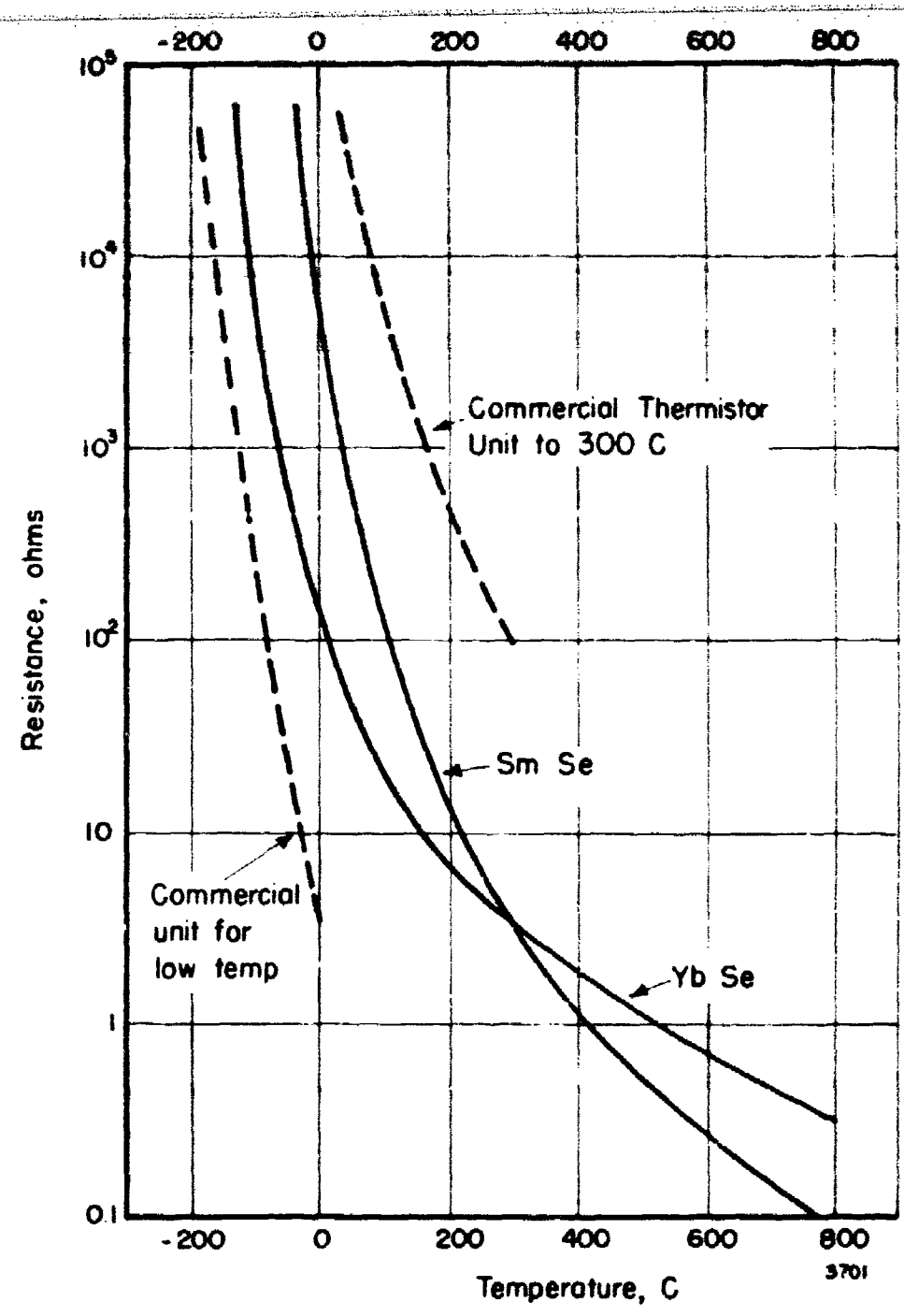

FIGURE 23. SPECIFIC RESISTANCE AS A FUNCTION OF TEMPERATURE FOR RARE-EARTH MONOSELENIDES AND COMMERCIAL THERMISTOR COMPOSITIONS

The degree of reproducibility obtained in the preparation of the rare-earth compositions, coupled with the good thermal stability and large TCR, makes these materials still more attractive. The advantages seen for these materials over commercial thermistor materials are based on these points, as follows:

(1) Potential operation at higher temperatures

(2) Less extensive calibration for each device element, since properties are very insensitive to purity and crystalline state

(3) Less stringent production-process control, since purity and crystalline state need not be controlled precisely

(4) Improved stability as compared with that of ceramic compacts

(5) Faster response times, since thermal conductivities of the crystalline materials may be expected to be higher than those of the pressed oxide powders.

Adjustable TCR Resistors

Studies of the aforementioned pseudobinary alloys of the compounds point to potential application for the alloy materials as well. Electrical-property studies of the SmSe-NdSe alloys show that the temperature coefficient of resistance (TCR) for low NdSe concentrations is negative, being quite large for pure SmSe and decreasing as the NdSe concentration is increased, as shown in Figure 24. On the other hand, for high NdSe concentrations, the TCR is positive, increasing in magnitude as the NdSe concentration is increased further. Hence, it is suggested that alloy compositions could be obtained which exhibit a chosen (even zero) TCR over a relatively large temperature range. For this particular alloy system the TCR for a composition containing 16 per cent NdSe is negative over the temperature range of the data shown in Figure 24 and is about 1700 ppm/C at 25 C. At 24 per cent NdSe, the TCR is found to be about -1000 ppm/C at 25 C, and at 33 per cent NdSe, the TCR is positive and <200 ppm at 25 C. Hence, the lowest TCR near room temperature would be expected for compositions in the range 24 to 33 per cent NdSe.

An investigation of other alloy systems of the same type (perhaps involving sulfur instead of selenium) would be expected to yield higher resistivity material at the optimum composition (i.e., the composition showing a minimum TCR). Alternatively, it may be possible, upon further study of such systems to tailor the TCR of the material to fit requirements for various applications and in various temperature ranges.

Thermoelectric Generators

Material in the group of rare-earth selenides and tellurides with compositions having metal-to-metalloid ratios in the range 3/4 to 2/3, and which crystallize in the Th_3P_4 structure, are of interest with respect to energy-conversion technology utilizing thermoelectric phenomena at high temperatures. Electrical resistivity and Seebeck

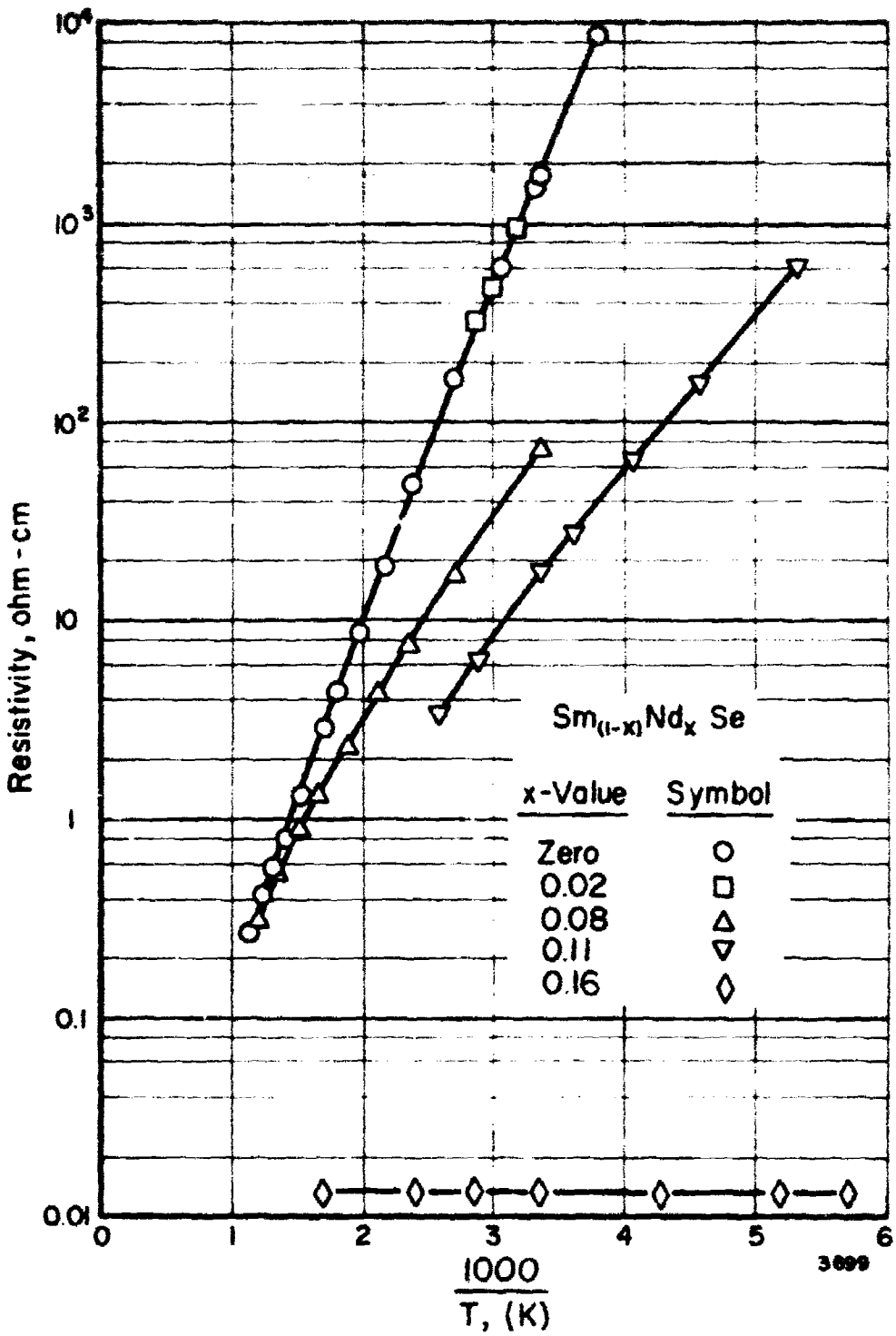

FIGURE 24. RESISTIVITY AS A FUNCTION OF TEMPERATURE FOR SmSe-NdSe ALLOYS

coefficient of these materials can be controlled by adjusting the metal-to-metalloid ratio and by replacing a portion of the rare-earth atoms with those of the alkaline-earth elements (calcium, strontium, barium). Table 14 shows thermoelectric data at 298 and 1300 K for representative compositions. Realizing that no serious attempt has been made to optimize these materials, estimated values of the dimensionless figure of merit ZT at 1300 K are extremely encouraging, being on the order of unity for a number of compositions already studied. As mentioned earlier, compositions lying within the cross-hatched area of Figure 15 may be expected to be especially attractive in this regard and should be investigated thoroughly.

Metal-Insulator Structures

The recent trend toward miniaturization of electronic components and circuitry has created intense interest in deposited-film microcircuitry, thus prompting interest in the so-called "tunnel emission" devices (Refs. 19-22) as potentially useful active components, which conveniently are prepared in thin-film form. These devices, which act as nonlinear conductors in a diode configuration and are capable of amplification in multielectrode configurations, are basically metal-insulator sandwiches, in which electrons pass through a thin insulator between metals by tunneling or by other mechanisms.

Although it is premature to suggest that rare-earth metals and oxides will be important materials for such devices, one may consider them as potentially useful. As indicated in the section on "Thin Films" (1) the rare-earth metals can be deposited as thin films, (2) thin rare-earth oxides can be formed on the metals by conventional techniques, such as, by anodization and vapor-phase reaction, (3) the rare-earth oxides appear to be suitably insulating materials, and (4) nonlinear conduction has been observed in metal-oxide-metal diode configurations.

SUMMARY

A considerable amount of progress has been made on the subject program in the synthesis and evaluation of new rare-earth compounds and compositions. More than 70 compounds and compositions (principally the rare-earth selenides, tellurides, and arsenides) have been prepared and studied in bulk and thin-film forms. The rare-earth compounds investigated are refractory materials having melting points in the range 1400 to 2200 C for the selenides, tellurides, and antimonides and in exess of about 2500 C for the arsenides, phosphides, nitrides, and oxides. The rare-earth metals are found to be quite reactive, particularly in the liquid state, hence finding suitable container materials for synthesis work was a problem. In addition, most of the reactions involved in syntheses at high temperatures were found to be rapid and exothermic. In general, both problems were surmounted by utilizing solid-vapor reactions at relatively low temperatures (400 to 1000 C). Methods have been developed for the growth of single crystals of the refractory compounds, both from the melt and from the vapor phase.

It has been found that, within a single system, MX_n, of variable selenium or tellurium content, a sequence of compounds can be formed, possessing a wide range of properties. In some ranges of composition, the transition from one type of conduction process to another appears to be gradual, thus presenting the opportunity for study of subtle differences between the extremes. When the changes in conductivity mechanism are accompanied by changes in structure, the opportunity exists, within a single binary system, for a study of the effects of changes in lattice spacing, bonding, and other crystalline environmental factors, on the transport properties of a solid. Complications resulting from changing chemical species are avoided. Thus, these are attractive systems for studying interrelations between crystal structures, band structures, and transport mechanisms.

Utilization of representative rare-earth elements to form compounds and alloys with the Group V-A and Group VI-A elements has provided materials for which electrical characteristics range from those of high-resistivity semiconductors to those of metal-like conductors, and which exhibit electronic transport properties of both practical and theoretical interest. It has been shown that the monoselenides and monotellurides of samarium and ytterbium are potentially valuable thermistor materials which can serve as a basis for the development of an improved device operable at high temperatures. Alloying these compounds with the monoselenides and monotellurides of tripositive rare-earth elements yields, within a given alloy system, specimens having resistivities in a wide range (10^{-5} to 10^{4} ohm-cm). In addition, within a given alloy system, one has control of the temperature coefficient of resistance, being able to vary it from negative to positive and apparently the ability to obtain a TCR very near zero over a wide temperature range. Analysis of electron conduction in these alloy systems indicates that the conduction process involves interactions between the tripositive rare-earth atoms in chainlike arrays on nearest-neighbor cation sites.

Results obtained have indicated that neodymium telluride and alloys of certain rare-earth and alkaline-earth selenides and tellurides are superior high-temperature thermoelectric generator materials which may be useful for energy conversion.

Metal-insulator configurations have been prepared with rare-earth metals and rare-earth oxides and analyzed electrically using diode structures. Electron transport through thin layers of the oxides has been observed and current-voltage characteristics consistent with tunneling have been observed qualitatively.

RECOMMENDATIONS

Results of this research have clearly shown the rare-earth metals and compounds to be interesting and potentially valuable materials worthy of further consideration and study as solid-state electronic materials. Four general types of future investigations are recommended:

(1) Device development programs based on potentially useful properties already observed

(2) Fundamental studies of transport phenomena and properties, band structures, and crystal structures of the materials.

(3) Continued exploratory study of the bulk properties of the materials, moving into study of other classes of compounds

(4) Continued exploratory study of the materials in thin films and thin-film structures, an area which has barely been entered.

It is believed that the cited results and accomplishments clearly indicate the desirability of continuing research on rare-earth metals and compounds for electronic applications. In addition to the section in this report which points out potential device applications, somewhat detailed recommendations on the development of thermistor or thermistor-type, adjustable-TCR-resistor, and thermoelectric-generator devices based on rare-earth selenides and tellurides previously have been submitted to the Electronic Technology Laboratory; these recommendations are reiterated here.

As is indicated in the Summary above, MX_n binary systems are attractive as the subjects of fundamental studies of crystal structures, band structures, and transport mechanisms. Such studies are recommended to advance the basic knowledge and understanding of the solid state.

Although good progress has been made, a number of rare-earth compounds containing Groups V and VI elements (e.g., oxides and phosphides) deserve more study of the general evaluation type. In addition, the solid-state electronic properties of rare-earth borides, silicides, and possibly carbides are of potential interest, and these compounds ultimately should be studied. With the amount of data generated in the past few years at Battelle and with the stimulated interest in rare-earth research at other laboratories, one has a good foundation on which to base choices of other rare-earth materials for more extensive research and development.

The observation of characteristics consistent with tunneling in rare-earth metal-oxide-metal structures, and the observed insulating properties of the oxide point to the desirability of continuing study of such materials in these structures and of continuing study of rare-earth materials in thin-film form. In this and in other cases, it appears that the low purity of the rare-earth materials and the presence of grain boundaries is now, or ultimately will be, factors limiting development of basic knowledge and potential use of the materials. Hence, it is recommended that emphasis be placed on the purification and control of the crystalline state of the rare-earth metals and compounds in future research, and particularly in the research on thin films.

PAPERS, PUBLICATIONS, AND PATENTS

To provide timely and fruitful dissemination of technical information generated on the program, numerous technical papers have been presented orally and published. Patent applications have been filed for two inventions made during the program and are entitled "Temperature Sensitive Devices" and "Resistance Devices". Papers presented and publications resulting from the subject investigations are listed, as follows:

Miller, J. F., and Himes, R. C., "Rare-Earth Intermetallic Compounds with Elements of Groups V and VI", presented at First Symposium on Rare Earth Research Developments, Lake Arrowhead, California, October, 1960.

Miller, J. F., and Himes, R. C., "Rare-Earth Intermetallic Compounds with Elements of Groups V and VI", Rare Earth Research, Edited by E. V. Kleber, The Macmillan Company, New York, 1961

Miller, J. F., Matson, L. K., and Himes, R. C., "Studies on the Selenides and Tellurides of Selected Rare-Earth Metals", presented at Second Symposium on Rare Earth Research Developments, Glenwood Springs, Colorado, September, 1961.

Miller, J. F., Matson, L. K., and Himes, R. C., "Studies on the Selenides and Tellurides of Selected Rare-Earth Metals", Rare Earth Research, Edited by J. Nachman and C. Lundin, Gordon and Breach Science Publishers Inc., New York, 1962.

Reid, F. J., Matson, L. K., Miller, J. F., and Himes, R. C., "Rare Earth Compounds for Thermoelectric Energy Conversion", presented at the Electrochemical Society Meeting, Boston, September, 1962.

Reid, F. J., Matson, L. K., Miller, J. F., and Himes, R. C., "Electrical Properties of Compounds and Alloys of Rare-Earth Metals with Elements of Groups V and VI", presented at the Electrochemical Society Meeting, Pittsburgh, April, 1963.

Miller, J. F., Matson, L. K., and Himes, R. C., "Observations on M_3X_4-M_2X_3 Crystalline Phases of Rare-Earth Tellurides, Selenides, and Sulfides presented at Third Symposium on Rare Earth Research Developments, Clearwater, Florida, September, 1963.

Reid, F. J., Matson, L. K., and Miller, J. F., "Electrical Properties of Refractory Rare Earth Monoselenides and Monotellurides", presented at the Electrochemical Society Meeting, New York, September, 1963.

Matson, L. K., Reid, F. J., and Himes, R. C., "Discussion of Electrical Conduction in SmSe-NdSe Alloys", presented at the Electrochemical Society Meeting, New York, September, 1963.

Miller, J. F., Matson, L. K., and Himes, R. C., "Observations on M_3X_4-M_2X_3 Crystalline Phases of Rare-Earth Tellurides, Selenides, and Sulfides", Rare Earth Research, Edited by J. Nachman and C. Lundin, Gordon and Breach Science Publishers, New York (to be published 1964).

Reid, F. J., Matson, L. K., Miller, J. F., and Himes, R. C., "Electrical Properties of Selected Rare-Earth Compounds and Alloys" (to be submitted for publication).

Reid, F. J., Matson, L. K., Miller, J. F., and Himes, R. C., "Electrical Properties of Refractory Rare-Earth Monoselenides and Monotellurides and Their Alloys" (to be submitted for publication).

REFERENCES

1) Miller, J. F., Reid, F. J., and Himes, R. C., J. Electrochem. Soc., 106 1043 (1959).

2) Stambaugh, E. P., Miller, J. F., and Himes, R. C., "Growth of Refractory III-V Compounds and Alloys From Solution", Metallurgy of Elemental and Compound Semiconductors, Edited by R. O. Grubel, Interscience Publishers, New York (1961).

3) Iandelli, A., Rare Earth Research, Edited by E. V. Kleber, The Macmillan Company, New York (1961), p 135.

4) Gschneidner, K. A., Jr., Rare Earth Alloys, D. Van Nostrand Company, Inc., Princeton, New Jersey (1961).

) Vickery, R. C., and Muir, H. M., "Observations on Some Gadolinium-Selenium Compounds", Rare Earth Research, Edited by E. V. Kleber, The Macmillan Company, New York (1961).

) Templeton, D. H., and Dauben, C. H., J. Am. Chem. Soc., 76, 5237 (1954).

) Pauling, L., J. Am. Chem. Soc., 69, 542 (1947).

) Pauling, L., The Nature of the Chemical Bond, 2nd Ed., Cornell University Press, Ithaca, New York (1945).

) Carter, F. L., Miller, R. C., and Ryan, F. M., Advanced Energy Conversion, 1, 165 (1961).

) Heikes, R. R., "Theory of the Electron-Transport Properties of the 4f Electrons in Rare Earth Compounds", Rare Earth Research, Edited by E. V. Kleber, The Macmillan Company, New York (1961).

) See, for example, Spedding, F. H., and Daane, A. H., The Rare Earths, John Wiley and Sons, Inc., New York (1961).

) Appel, J., Phil. Mag., 6, 167 (1961).

) Miller, R. C., and Ure, R. W., Jr., Energy Conversion for Space Power, Edited N. W. Snyder, Academic Press, New York (1961).

) Kurnick, S. W., Fitzpatrick, R. L., and Merriam, M. F., "Physical Properties of Barium-Doped Cerium Sulfide", Rare Earth Research, Edited by J. F. Nachman and C. E. Lundin, Gordon and Breach Science Publishers, Inc., New York (1962).

Kubaschewski, O., and Hopkins, B. E., Oxidation of Metals and Alloys, Academic Press, London (1962).

(16) Chang, N. C., J. Appl. Phys., 34, 3500 (1963).

(17) Meyerhofer, D., and Ochs, S. A., J. Appl. Phys., 34, 2535 (1963).

(18) Simmons, J. G., J. Appl. Phys., 34, 1793 and 2581 (1963).

(19) Mead, C. A., J. Appl. Phys., 32, 646 (1961).

(20) Hickmott, T. W., J. Appl. Phys., 33, 2669 (1962).

(21) Kanter, H., and Feibelman, W. A., J. Appl. Phys., 33, 3580 (1962).

(22) Erntage, P. R., and Tantraporn, W., Phys. Rev. Letters, 8, 267 (1962).

JFM:dnm